ResearchGate

See discussions, stats, and author profiles for this publication at: https://www.researchgate.net/publication/387531339

Repurposing antiviral drugs targeting the PARP-1 and HER2 pathways with multifaceted impacts through integrated network analysis and molecular mechanics

Article *in* Chemical Physics Impact · December 2024

DOI: 10.1016/j.chphi.2024.100812

CITATIONS
0

READS
88

3 authors, including:



Praveen Sekar
Swamy Vivekanandha College of Pharmacy, Tiruchengode, Namakkal, Tamilnadu, India
46 PUBLICATIONS **177** CITATIONS

SEE PROFILE

All content following this page was uploaded by Praveen Sekar on 06 January 2025.

The user has requested enhancement of the downloaded file.

Chemical Physics Impact 10 (2025) 100812

Contents lists available at ScienceDirect

Chemical Physics Impact

journal homepage: www.sciencedirect.com/journal/chemical-physics-impact

Full Length Article

Repurposing antiviral drugs targeting the PARP-1 and HER2 pathways with multifaceted impacts through integrated network analysis and molecular mechanics

Uma Maheshwari Mugundan [a], Praveen Sekar [b], Rajanandh Muhasaparur Ganesan [a,*]

[a] Department of Pharmacy Practice, SRM College of Pharmacy, SRM Institute of Science and Technology, Kattankulathur, Chengalpattu, 603203, Tamilnadu, India
[b] Department of Pharmaceutical Chemistry, Swamy Vivekanandha College of Pharmacy, Tiruchengode, 637205, Tamilnadu, India

ARTICLE INFO

Keywords:
Breast cancer
Drug repurposing
Anti-cancer
Network pharmacology
Molecular simulations

ABSTRACT

This study investigates the anticancer potential of existing anti-viral drugs using a comprehensive suite of computational methods. A dataset of 76 antiviral drugs was prepared and optimized for analysis. Through the application of network pharmacology, gene ontology, and Kyoto Encyclopedia of Genes and Genomes (KEGG) pathway enrichment analyses, this study identified Human Epidermal Growth Factor Receptor 2 (HER2) and Poly [ADP ribose] polymerase 1(PARP-1) as key targets involved in the molecular pathways associated with breast cancer. Protein sequence alignment further revealed conserved and semi-conserved amino acid regions, including residues such as Arginine (ARG), Aspartic acid (ASP), and Phenylalanine (PHE), offering valuable insights into the structural characteristics of the target proteins. Molecular docking studies were performed to evaluate drug-receptor interactions, leading to the selection of promising candidates: Fostemsavir, Efavirenz, Doravirine, and Didanosine for HER2, and Efavirenz, Lopinavir, Fostemsavir, and Elvitegravir for PARP-1. The binding affinities observed were -7.92 Kcal/mol for HER2 and -8.08 Kcal/mol for PARP-1 for Efavirenz, and -8.17 Kcal/mol for HER2 and -7.91 Kcal/mol for PARP-1 for Fostemsavir. Subsequent molecular dynamics simulations, conducted over 200 ns, assessed the stability of these drug-protein complexes. Binding free energy was calculated using Molecular Mechanics/Generalized Born Surface Area (MM-GBSA) methods, reinforcing the stability and efficacy of the selected compounds followed by entropy calculation using Normal mode analysis done for Efavirenz complexes. Results of this study demonstrated that Efavirenz exhibits strong binding and notable potential as HER2 and PARP-1 inhibitors. Efavirenz demonstrated effectiveness against both targets, emphasizing its potential and showcasing drug repurposing as a promising strategy in cancer therapy development.

Introduction

Breast cancer continues to pose a significant global health challenge, resulting in approximately 670,000 fatalities and impacting 2.3 million individuals in 2022. The incidence of breast cancer is notably influenced by the Human Development Index (HDI), with 1 in 12 women in high-HDI countries facing a lifetime diagnosis risk, and 1 in 71 at risk of mortality from the disease [1]. In India, among women, breast cancer is the most prevalent malignancy representing 28 % of all cancers among the female population, with an estimated 216,108 new cases reported in 2022 [2]. The lifetime risk of developing breast cancer for women in the general population ranges from 1 in 8 to 12 [3,4]. The diverse phenotypic characteristics of breast cancer complicate treatment strategies, as each subtype displays distinct biological and clinical traits [5]. These subtypes are categorized based on hormonal receptor status: Estrogen receptor (ER) positive, Progesterone receptor (PR) positive, Human Epidermal Growth Factor Receptor 2 (HER2) positive, and Triple-negative breast cancer (TNBC). HER-2-positive and TNBC are among the most aggressive subtypes of breast cancer, contributing significantly to mortality due to their rapid progression and limited therapeutic options [6,7].

HER-2-positive breast cancer is characterized by overexpression of the HER-2 protein, constitutes 20–30 % of all breast cancer cases, and is associated with unfavorable outcomes and elevated recurrence rates [8]. HER2-enriched tumors typically have a poorer prognosis; however, they often show improved responses to biological therapies when used in

* Corresponding author.
E-mail address: mgr@srmist.edu.in (R. Muhasaparur Ganesan).

https://doi.org/10.1016/j.chphi.2024.100812
Received 29 September 2024; Received in revised form 8 December 2024; Accepted 28 December 2024
Available online 30 December 2024
2667-0224/© 2025 The Authors. Published by Elsevier B.V. This is an open access article under the CC BY license (http://creativecommons.org/licenses/by/4.0/).

conjunction with chemotherapy [9]. Targeting HER-2 has revolutionized treatment for this subtype, but resistance to existing therapies and recurrence remain critical challenges. Consequently, we chose to study HER-2 directly to explore novel therapeutic strategies that could enhance outcomes in this high-risk group [6,7].

TNBC is defined by the absence of ER, PR, and HER-2 expression, which lacks targeted treatment options, making it particularly challenging to manage. TNBC represents about 10–15 % of all breast cancer cases and it is known for its aggressive nature with a poorer prognosis. Among the potential molecular targets for TNBC, PARP-1 (poly ADP-ribose polymerase-1) has emerged as a promising candidate. TNBC tumors, especially those with BRCA1/2 mutations, often exhibit deficiencies in homologous recombination repair, making them highly dependent on PARP-1 for DNA damage repair. Inhibiting PARP-1 in such tumors leads to synthetic lethality, overwhelming the tumor's DNA repair mechanisms and inducing cell death [10–12]. Recognizing the therapeutic relevance of PARP-1 in TNBC, we selected it as a key focus of our study to address the pressing need for more effective targeted therapies in this aggressive subtype.

Despite significant advancements in breast cancer therapies, there remains an urgent demand for innovative and cost-effective treatment strategies, particularly for aggressive subtypes such as HER2-positive and TNBC. Drug repurposing presents a viable solution by utilizing the known safety and pharmacokinetic profiles of existing medications, thereby accelerating the drug discovery process [13]. Notably, antiviral agents have exhibited potential anticancer properties, with evidence suggesting a reduction in cancer-related mortality among patients undergoing antiretroviral therapy. Repurposing antiviral drugs as potential anticancer agents offers a compelling strategy to address the challenges associated with developing novel therapeutics.

Antiviral drugs are designed to target highly conserved enzymes and pathways essential for viral replication, many of which overlap with mechanisms crucial for cancer cell survival and proliferation. This shared biology provides a strong rationale for exploring antivirals in oncology [14]. Furthermore, antivirals possess well-established safety profiles, and pharmacokinetics, significantly reducing the time and cost associated with drug development [15,16].

The justification for this approach lies in the growing evidence that some antivirals can modulate cancer-specific targets, disrupt DNA repair mechanisms, or induce metabolic stress in cancer cells. However, the potential of antivirals to inhibit proteins like HER-2 and PARP-1 has not been thoroughly investigated, the graphical representation of the HER2 pathway and PARP-1 pathway is given in Fig. 1. By studying the interactions of these drugs with HER-2 and PARP-1 using advanced computational techniques, our research seeks to provide novel insights into their potential repurposing for breast cancer treatment, particularly in addressing unmet therapeutic needs in HER-2-positive and TNBC subtypes [17–21].

Experiments and methodology

Mechanistic target prediction using network pharmacology

Aggregation of targets

To identify potential molecular targets for the compound, we performed mechanistic target prediction using network pharmacology. This approach provides a thorough analysis of how the compound interacts within biological networks, revealing potential pathways and processes it may influence, thereby enhancing our understanding of its therapeutic potential. Initially, the targets of the anti-retroviral drugs were predicted using the SWISS Target Prediction and SuperPred web servers. Genes associated with breast cancer were sourced from the Genecards and OMIM databases. The overlapping common genes from the predictions were identified by generating a Venn diagram using the Venny database [22,23].

Construction of protein-protein interaction network

We created a protein-protein interaction (PPI) network to illustrate the interactions between targets. This analysis offers valuable insights into the interrelated functions of target proteins, their downstream effects, and the broader systemic implications of modulating specific proteins. The PPI network for the common genes identified from the Venn diagram was constructed using the STRING database, with Homo sapiens selected as the test organism and a minimum interaction score of

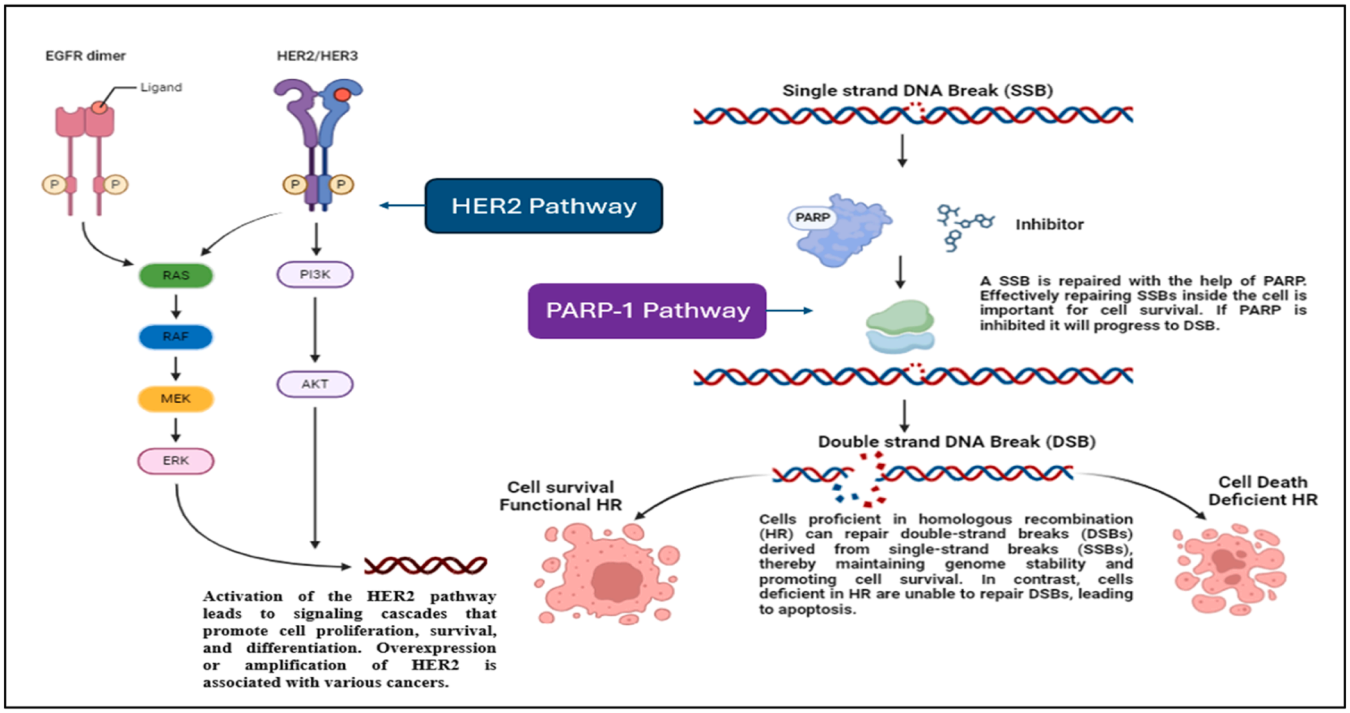

Fig. 1. Diagrammatic representation of the HER2 pathway and PARP-1 pathway.

0.4. The aim of creating a minimal interaction network was to streamline future research efforts using Cytoscape [22,24].

Visualization of network

To enhance the interpretation of complex protein relationships, we visualized the interaction network. This graphical representation facilitates the identification of key nodes and highlights crucial proteins that may play significant roles in disease pathways. The networks were constructed using Cytoscape, a powerful software tool for network visualization. Additionally, web-based resources such as the STRING database were utilized to seamlessly export specific networks. As noted by Shannon et al. (2003), fundamental grid networks were employed to predict targets and identify the network responsible for addressing breast cancer. By utilizing target prediction and network pharmacology techniques, we analyzed the most prominent pathways and targets, enabling the selection of potential targets for further biological investigation [24].

Functional enrichment analysis of Gene Ontology (GO) and KEGG pathways

We performed an in-depth functional enrichment analysis of Gene Ontology (GO) terms and Kyoto Encyclopedia of Genes and Genomes (KEGG) pathways to gain functional insights. This approach elucidates the molecular functions, biological processes and cellular components linked to the identified targets, while also highlighting relevant pathways that could indicate the compound's mechanisms of action or potential side effects. The GO and KEGG pathway enrichment analysis of common genes from the Venn diagram was performed using the ShinyGO 0.80 tool, providing detailed annotations based on Biological Process, Cellular Component, KEGG and Molecular Function.

In the Gene Ontology framework, the Biological process outlines the physiological or cellular functions associated with the selected genes, while cellular component details the localization of gene products within the cell to facilitate their activities. Molecular Function refers to the specific biochemical activities of the selected genes. KEGG integrates chemical, genetic, and systemic functional data, offering insights into complex biological functions and applications at the molecular level [23,25]. The tool generates plots of the enriched genes, categorized according to their functional significance.

Construction and analysis of cluster GO and KEGG enrichment network

We developed and examined a clustered network for GO and KEGG enrichment analysis. This organized clustering method groups related biological functions and pathways, allowing for the identification of prominent themes and processes shared among the targets. The functional enrichment network for the shared targets was constructed using GO Biological Process and KEGG pathway data through the ClueGO plugin within Cytoscape software. This tool visualizes the molecular mechanisms of the common genes implicated in breast cancer, presenting the data in both network charts and pie charts [26–28]. To ensure the robustness of the findings, signaling pathways, network charts, and results from both enrichment analyses were cross-referenced and compared for consistency and reliability.

Protein-ligand preparation

To ensure precise docking simulations, thorough preparation of the protein-ligand complexes was conducted. This preparatory step refines the protein structures and optimizes the ligand conformations, thereby enhancing the reliability of predicted binding affinities and interactions. For our study, the target proteins PARP (PDB ID: 5LX6 having a resolution of 1.25 Å) and HER2 (PDB ID: 3PP0 having a resolution of 2.25 Å) were chosen based on curated literature and refinement scores, and protein preparation is carried out by addressing any missing atoms or residues and non-essential components, such as water molecules and co-crystallized ligands, were removed to prevent interference during docking. Hydrogen atoms were added to the protein, with particular attention to the protonation states of ionizable residues. Finally, energy minimization was performed to resolve steric clashes and optimize the protein structure.

Regarding ligand preparation, 76 drug molecules were initially sketched in 2D using ChemDraw 16.0, followed by their conversion to 3D structures using Chem3D Pro. The ligands then underwent energy minimization using the Avogadro cross-platform molecular editor, ensuring optimal geometry and stability. The minimized compounds were saved in SDF format, ready for further analysis.

Protein sequence alignment

We conducted protein sequence alignment to evaluate similarities across various protein sequences. This analysis is essential for confirming target specificity and identifying potential off-target interactions, ensuring the selection of appropriate homologous models for molecular docking or simulations. Protein sequence alignment is a critical process in bioinformatics that allows for the comparison and assessment of similarities and differences between multiple sequences. In our study, we focused on analyzing the sequence alignment between retroviral proteins and cancer-associated proteins to assess sequence similarities—a key aspect of our drug repurposing methodology. Identifying these regions of similarity aids in understanding the functional, structural, and evolutionary relationships between the sequences.

For the analysis, we provided a FASTA file as the input sequence. Although there are numerous algorithms available for protein sequence alignment, each with distinct advantages and limitations, we opted for the ClustalW/Clustal Omega algorithm due to its high accuracy. This algorithm employs seeded guide trees and hidden Markov model (HMM) profile-profile techniques to produce reliable alignments, making it suitable for medium to large-scale analyses. The aligned sequences were subsequently refined and examined, allowing us to derive insights for phylogenetic analysis, pinpoint conserved regions, and predict protein structures or functions—findings that are vital for the subsequent stages of our research [29–31].

Molecular docking analysis

Molecular docking was done to predict the binding mode and affinity of the compound with its target proteins, providing molecular-level insights into interactions and aiding the prioritization of lead compounds based on binding energy and interaction profiles. Molecular docking has evolved as an essential tool for lead compound discovery and optimization . In this study, molecular docking was executed using the AutoDock 4.2 program, targeting PARP and HER2 proteins. The 3D crystal structures of PARP (PDB ID: 5LX6) and HER2 (PDB ID: 3PP0) were retrieved from Protein data bank, chosen for their high resolution, lower R-values, and minimal Ramachandran plot outliers. The protein structures were refined by removing water molecules and heteroatoms [32–35]. Protonation in 3D was performed to enhance sensitivity to electronegative atoms. Protein structures were energy minimized, which was carried out as part of the preparation for molecular docking. The docking analysis employed the 2022 version of the AutoDock 4.2 software, where ligand molecules were optimized using Avogadro - the advanced molecular editor software and subjected to energy minimization using the Amber 10:EHT force field . The best binding modes were determined using the Lamarckian genetic algorithm, with ten conformations generated for each compound. The top-ranked conformation, featuring an Root Mean Square Deviation (RMSD) value of <2 Å, was selected for further analysis. Ligand-receptor interactions were visualized in both two-dimensional (2D) and three-dimensional (3D) representations [36–45].

ADMET analysis

Drug-likeness analysis is a crucial step in lead compound discovery, as many candidates fail in clinical trials due to inadequate ADME properties and potential toxicity in biological systems. A drug's pharmacological effectiveness is largely influenced by its physicochemical properties, including rotatable bonds, topological polar surface area,

and the presence of hydrogen bond acceptors and donors. Many approved drugs adhere to Lipinski's Rule of Five, a guideline indicating whether a compound is likely to have good oral bioavailability, along with supporting other pharmacokinetic considerations such as ADME properties. ADME studies were performed using the SwissADME online predictor, while Molinspiration, another online tool, was utilized to evaluate bioactivity and pharmacokinetic parameters [46].

Molecular dynamics simulation

Molecular dynamics (MD) simulations were performed to evaluate the stability of the compound-protein complex under simulated physiological conditions. This approach reveals conformational changes, binding stability, and the dynamic interactions that static docking cannot capture. MD simulations were carried out for the top compounds of docking studies Efavirenz, Fostemsavir, Doravirine, Didanosine, Lopinavir and Elvitegravir using the Desmond Version 5.9 Package from Schrödinger LLC. Initially, the HER2 and PARP docked complex was refined using the OPLS force field, and an orthorhombic cubic simulation box was prepared with the complex centered within it. TIP3P water molecules and buffers were added to maintain an approximate 10 Å distance between the protein atoms and the box walls. To set up the system, Na+ and Cl- counter ions were introduced, and the box volume was adjusted accordingly.

System minimization was performed using the OPLS-2005 force field parameters within the Desmond protocol. The simulation maintained a Berendsen NVT ensemble with a temperature restraint of 10 K on the solute's heavy atoms. The main simulation was conducted at 300 K and 1 atmosphere of pressure, using a relaxation time of 20 ps to ensure the temperature remained constant at 300 K and pressure remained constant at 1 atm. The Martyna-Tobias-Klein barostat and Nosé-Hoover thermostat were employed for pressure and temperature control, respectively. The simulation, which lasted approximately 200 ns, was conducted under an NPT ensemble. Frames were extracted throughout the simulation, and simulation interaction diagrams were generated to meticulously analyze trajectory fluctuations [47–49].

Free energy calculations

We conducted binding free energy calculations to quantitatively evaluate the binding affinity between the compound and the target protein. This analysis is pivotal for validating the binding efficiency predicted through docking and for directing subsequent optimization of potential drug candidates. The binding free energies of the protein-ligand interactions were assessed using the MM-GBSA method. The Prime-MM/GBSA tool within the Maestro suite was utilized for these calculations on selected complexes, five fundamental energy calculations are done using Prime MM-GBSA:

Optimized free receptor (="Receptor")
Optimized free ligand (="Ligand")
Optimized complex (="Complex")
Receptor from minimized/optimized complex
Ligand from minimized/optimized complex.

From these energies, the following strain and binding energies are calculated:

MMGBSA dG Bind (ΔG_bind) = Complex − Receptor − Ligand
MMGBSA dG Bind (ΔG_bind) (NS) = Complex − Receptor(from optimized complex) − Ligand(from optimized complex) = MMGBSA dG Bind − Rec Strain − Lig Strain.

In this approach, a limited number of snapshots were used from a 200 ns molecular dynamics (MD) simulation, in comparison to the typical model window of 1000 snapshots. The molecular mechanics energies of the OPLS force field and the variable dielectric Generalized Born (VSGB 2.0) solvation model were employed to account for the solvation effects of polar substances. Non-polar solvation effects were addressed through the Solvent-Accessible Surface Area (SASA) and Van der Waals contributions calculated by Prime-MMGBSA. This combined methodology yields the ΔG_bind values within the complex throughout molecular dynamics simulations [50–54].

Normal mode analysis

Normal mode analysis (NMA) was performed for the protein complexes to estimate the vibrational entropy contributions using the ElNémo web server (https://www.sciences.univ-nantes.fr/elnemo/start.html) [55]. The input structure was prepared by removing water molecules and other irrelevant entities and energy minimization to ensure a stable conformation. The protein structure was submitted in PDB format to ElNémo, and default parameters were used for the calculations.

Low-frequency normal modes, which represent collective motions within the protein, were analyzed. Entropy contributions (TΔS) were estimated from these low-frequency modes using their computed frequencies. The following formula was employed to compute the vibrational entropy:

$$S = R\sum_i \left[\frac{h\nu_i/k_BT}{\exp(h\nu_i/k_BT)-1} - \ln(1-\exp(-h\nu_i/k_BT))\right]$$

Where R is the Gas constant (8.314 J/mol\cdotpK), h is Planck's constant (6.626 × 10−34 J\cdotps), Boltzmann constant (kB = 1.38 × 10−23 J/K), T: Absolute temperature (e.g., 298.15 K). ν_i are the normalized frequencies of the selected modes 7–20, the total vibrational entropy of the system was then expressed in kcal mol^{-1} K^{-1}. This calculation captures the contributions of the collective motions of the protein-ligand system and provides insights into the complex's flexibility and dynamic properties [56].

Principal component analysis

Principal Component Analysis (PCA) was employed to investigate the collective movements within the protein complexes using the trajectories collected from the dynamics simulation, and the graph was plotted using MDtraj [57]. PCA, a dimensionality reduction technique, identifies the principal modes of motion within a system. By analyzing the first few eigenvectors (EVs), which represent the dominant modes of motion, the conformational dynamics of both complexes were examined throughout the simulation. The time evolution of PCA was employed to evaluate the overall flexibility of the Efavirenz-HER2 and Efavirenz-PARP complexes. The Lower overall flexibility observed in the primary EVs indicated a stable conformation for both complexes [58].

Results and discussion

Predicting therapeutic targets using network pharmacology approaches

Common genes acquisition

Antiviral medications that have been tested have shown a favorable response to many forms of cancer, according to the targets predicted by the SWISS Target Prediction and SuperPred databases. It was necessary to retrieve the targets/genes from the GeneCards and OMIM human databases to find the cancer-causing genes. With a probability greater than 0.09 for drug targets and >50 for disease targets, the most suitable genes were chosen from the obtained list of genes. Using the collected list as a basis, the 19 most common genes were identified using the Venn diagram; Fig. 2**A** displays the results.

Development and investigation of protein-protein interactions (PPI)

The networks were constructed by utilizing the bioactive targets of the newly generated query molecules. The next step is to identify targets linked to the shared pathway with cancer. Understanding the process underpinning targets and improving target visualization both

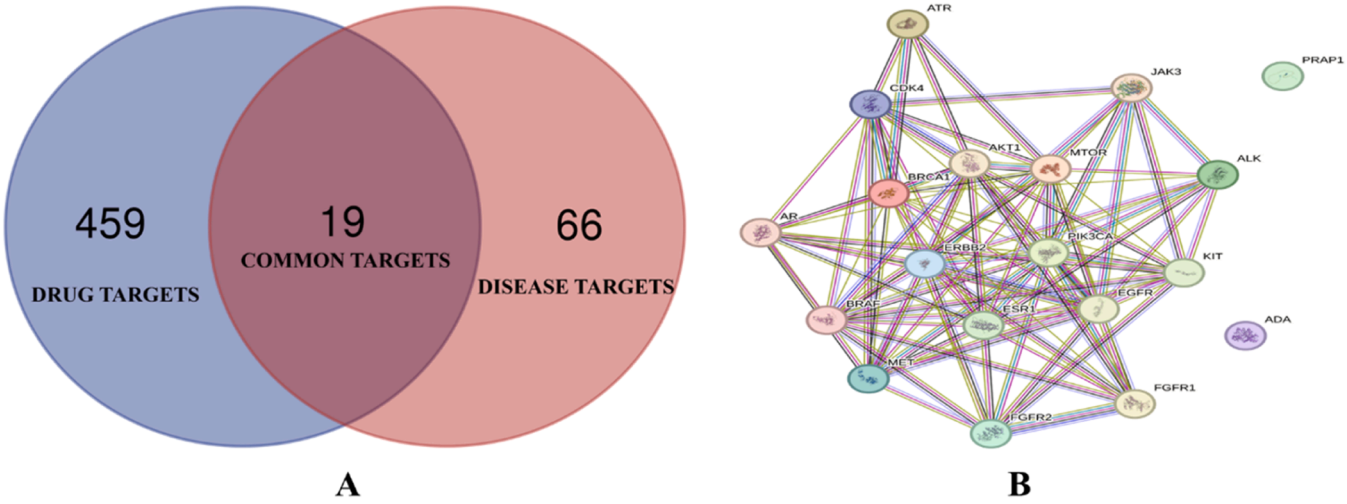

Fig. 2. Construction and analysis of network with Top 10 Targets; A) Venn Plot; B) PPI for designed compounds.

necessitate examining the PPI of the target genes. In order to construct the PPI network, we examined the target genes of the relevant components using STRING version 11.5. Fig. 2**B** shows the PPI network with 29 nodes and 61 edges, as shown in the STRING database. In this case, PPI serves as the edge and proteins as the nodes. A score level higher than 0.9 was used to set the data for the high-confidence target protein interactions. In addition to the number of targets linked to the network, the average node degree is 11.5 and the average local clustering coefficient is 0.729. The degree is a crucial statistic for illustrating the functioning of network nodes and protein interactions. In accordance with the PPI network, the genes namely ATR, CDK4, JAK3, PARP1, AKT1, ERBB2, MTOR, ALK, BRCA1, AR, PIK3CA, KIT, EGFR, ESR1, ADA, FGFR1, FGFR2, BRAF and MET are involved and interacted. The significant positioning of the breast cancer target isoforms within the interaction network supports the notion that proteins play a role in the process of breast carcinogenesis. The blue nodes are representative of the essential subnetwork or module that is involved in the process of molecular action. The hub proteins that are related with diseases make up the larger nodes. AKT1, ERBB2, EGFR, MTOR, PIK3CA, ESR1, PARP1 and JAK3 are all linked pathways that play a role in the therapy of cancer. The ERBB2 also known as HER2 protein, the family member of EGFR and ESR1 (Estrogen Positive-1) are the genes, whose overexpression plays a vital role in malignancies, especially breast cancer [59]. A key intracellular signaling pathway known as PI3K/Akt/mTOR has a well-established involvement in tumor cell growth and proliferation in response to hormone, nutritional, and growth factor stimulation. A member of the class IA PI3 K family, the PI3 K heterodimer is fundamental to this route. The regulatory subunit (p85) controls the activation of the catalytic subunit (p110) in the heterodimer based on the presence or absence of upstream stimulation by growth factor receptor tyrosine kinases (RTKs). mTOR is a protein kinase that is serine/threonine-dependent and is located downstream of Akt and PI3K. There is evidence that endocrine resistance is associated with the PI3K/Akt/mTOR pathway. According to preclinical research, Akt can activate the estrogen receptor (ER) pathway regardless of estrogen availability, and endocrine therapy resistance can be overcome by combining mTOR inhibitors with endocrine therapy. In HER2-overexpressing breast cancer, trastuzumab resistance has been linked to the PI3K/Akt/mTOR pathway [60,61]. The activation of the PI3 K pathway and impairments in DNA repair are rather prevalent occurrences in breast cancer. Novel medicines, such as poly (ADP-ribose) polymerase (PARP) inhibitors, are one example of a situation in which the production of double-stranded breaks in DNA results in the death of tumor cells that have a defect in homologous DNA repair [62]. Evidence from preclinical research suggests that these pathways are interlinked with the development of cancer. The results demonstrated that the designed compounds might inhibit the development of cancer cells through protein-protein interactions and thereby have the potential to limit cell proliferation, cell cycle arrest and apoptosis [63].

Construction and visualization of network

In order to enhance the visualization and study of PPI, the data that was retrieved was then loaded into the Cytoscape 3.10.0 software. This allowed for the construction of a new network, which also displays 29 nodes and 61 edges. The targets that were ideal for biological studies were then mined using the Cytohubba plugin program. We used the Cytohubba plugin software to uncover the top targets that the compounds are active against by analyzing the top 10 computations according to degree. Our results only proved that the three potential targets PARP1, ERBB2 and MTOR are very connected to one another. In cancer cells, PARP1 controls cell mitosis and several cell death mechanisms such necroptosis, apoptosis and necroptosis. In general terms, DNA repair pathways are the primary targets of the antineoplastic action exhibited by currently developed PARP1 inhibitors. The overexpression of HER2 is believed to lead to constitutive activation of the tyrosine kinase domain, which in turn activates downstream protein pathways, leading to dysregulated gene transcription (e.g., PIK3CA/AKT/mTOR and 81 RAS/RAF/MAPK). Researchers have focused on breast cancer to learn how HER2/neu overexpression affects PARPi activity. The results of various studies show that high HER2 expression may make breast cancer more sensitive to PARPi, independent of BRCA status, suggesting a potential alternative "BRCAness" mechanism. The capacity for homologous recombination (HR) mediated repair was considerably diminished by lapatinib, a dual tyrosine kinase inhibitor against HER1/HER2, in a study of breast cancer patients with HER2 overexpression (+). Targeting downstream of the HER2 receptor reduced BRCA1/2 and enhanced PARP activity, resulting to tumor sensitivity to PARPi, according to another study in breast cancer [64–66]. We also used the CytoNCA plugin of Cytoscape software to investigate the network's topology in detail. The distinct centrality measures offered by CytoNCA make it compatible with weighted biological networks. Additional biological properties could be examined and analyzed using CytoNCA to enhance the four centrality metrics that are already accessible. Table 1 shows the calculated values of degree, betweenness, closeness, and eigenvector centralities.

Enrichment analysis

The GO terms and KEGG pathways enrichment studies were carried out in order to acquire a large-scale comprehension of the functionalities of the common targets. As a consequence of this, a bar plot was used to

Table 1
Computed values of the network.

Target	Degree	Betweenness	Closeness	Eigenvector
ERBB2	14	6.695	0.888	0.278
PARP1	15	7.334	0.941	0.296
MTOR	15	12.520	0.941	0.288
BRCA1	15	12.477	0.941	0.292
ESR1	14	4.477	0.888	0.285
BRAF	13	3.759	0842	0.267
EGFR	14	6.007	0.888	0.279
AKT1	13	6.806	0.842	0.262
KIT	12	4.304	0.800	0.243
AR	11	0.770	0.761	0.241

visually represent the top ten most enriched GO terms in the areas of biological processes, cellular components, and molecular functions.

Further, the pathways associated with the targets were studied using the KEGG pathway analysis. Among the obtained pathways and enriched genes, the majority of the pathways showed that the tested genes are active breast cancer. The top 10 enriched GO terms and KEGG pathways along the description, number of genes and false discovery rate (FDR) are given in Table 2. From the obtained GO results, it came to know that the query molecules were involved in the regulation of programmed cell death, intracellular signal transduction, protein tyrosine kinase activity, serine/threonine/tyrosine kinase, ATP binding, receptor complex, Adenyl nucleotide binding, apoptosis and in different signaling pathways. The above findings showed that the compounds will act against breast cancer via the downregulation of serine/threonine/tyrosine kinase (AKT/PI3KCA/MTOR), ATP binding and Adenyl nucleotide binding (PARP1). The pathways involved in the KEGG analysis include EGFR tyrosine kinase inhibitor resistance, Breast cancer, Endocrine resistance, PI3K-Akt signaling pathway and different pathways in cancer. These results also proved the efficiency of the tested antiretroviral drugs against breast cancer [67,68]. The bar plots representing the enriched pathways obtained from GO and KEGG analysis are given in Fig. 3.

Enrichment analysis using ClueGO software

Using the obtained common list of genes, the enrichment analysis was again performed using the ClueGO plugin of the Cytoscape software to correlate the results of the ShinyGO 0.80 tool. The list of genes was uploaded in the plugin software and the top pathways associated with the test genes and query molecules were identified by setting Homo sapiens as the test organism and Benjamini-Hochberg as the statistical method. The pathways based on the KEGG and GO Biological processes were derived using the above criteria and the pathways and pie charts representing the top enriched pathways are given in Figs. 4–6.

The KEGG pathway clearly showed that the tested antiretroviral

Table 2
The Top 10 enrichment pathways of GO and KEGG analyses.

Go Biological Process			
GO Terms	Description	nGenes	False Discovery Rate (FDR)
GO:0,004,714	Transmembrane receptor protein tyrosine kinase signaling pathway	13	1.2E-13
GO:0,043,068	Reg. of programmed cell death	16	2.0E-13
GO:0,035,556	Reg. of intracellular signal transduction	17	7.6E-14
GO:0,012,501	Programmed cell death	16	5.6E-12
GO:0,035,556	Intracellular signal transduction	18	3.0E-13
GO:0,009,967	Reg. of signal transduction	19	7.6E-14
GO:0,010,649	Reg. of cell communication	19	2.4E-13
GO:0,010,469	Reg. of signaling	19	2.4E-13
GO:0,048,583	Reg. of response to stimulus	19	5.2E-12
Go Molecular Function			
GO:0,004,714	Transmembrane receptor protein tyrosine kinase activity	7	2.4E-12
GO:0,004,713	Protein tyrosine kinase activity	9	8.2E-14
GO:0,004,712	Protein serine/threonine/tyrosine kinase activity	14	3.9E-18
GO:0,004,672	Protein kinase activity	14	1.3E-16
GO:0,016,773	Phosphotransferase activity alcohol group as acceptor	14	8.9E-16
GO:0,016,301	Kinase activity	14	3.9E-15
GO:0,016,772	Transferase activity transferring phosphorus-containing groups	14	3.4E-14
GO:0,005,524	ATP binding	14	1.9E-11
GO:0,030,554	Adenyl nucleotide binding	14	2.9E-11
Go Cellular Component			
GO:0,016,021	Spanning component of plasma membrane	2	8.3E-03
GO:0,043,235	Receptor complex	7	5.4E-06
GO:0,009,925	Basal plasma membrane	3	1.9E-02
GO:0,007,043	Cell-cell junction	4	1.9E-02
GO:0,009,986	Cell surface	5	1.9E-02
GO:0,016,021	Integral component of plasma membrane	7	1.9E-02
GO:0,031,226	Intrinsic component of plasma membrane	7	1.9E-02
GO:0,031,410	Cytoplasmic vesicle	8	1.9E-02
GO:0,016,050	Vesicle	10	1.9E-02
KEGG			
hsa05230	Central carbon metabolism in cancer	9	6.2E-17
hsa05223	Non-small cell lung cancer	9	6.2E-17
hsa01521	EGFR tyrosine kinase inhibitor resistance	8	2.2E-14
hsa05218	Melanoma	7	1.7E-12
hsa05215	Prostate cancer	9	6.9E-16
hsa01522	Endocrine resistance	8	9.1E-14
hsa05224	Breast cancer	11	2.9E-18
hsa05205	Proteoglycans in cancer	9	4.0E-13
hsa04151	PI3K-Akt signaling pathway	12	2.2E-16
hsa05200	Pathways in cancer	15	1.3E-19

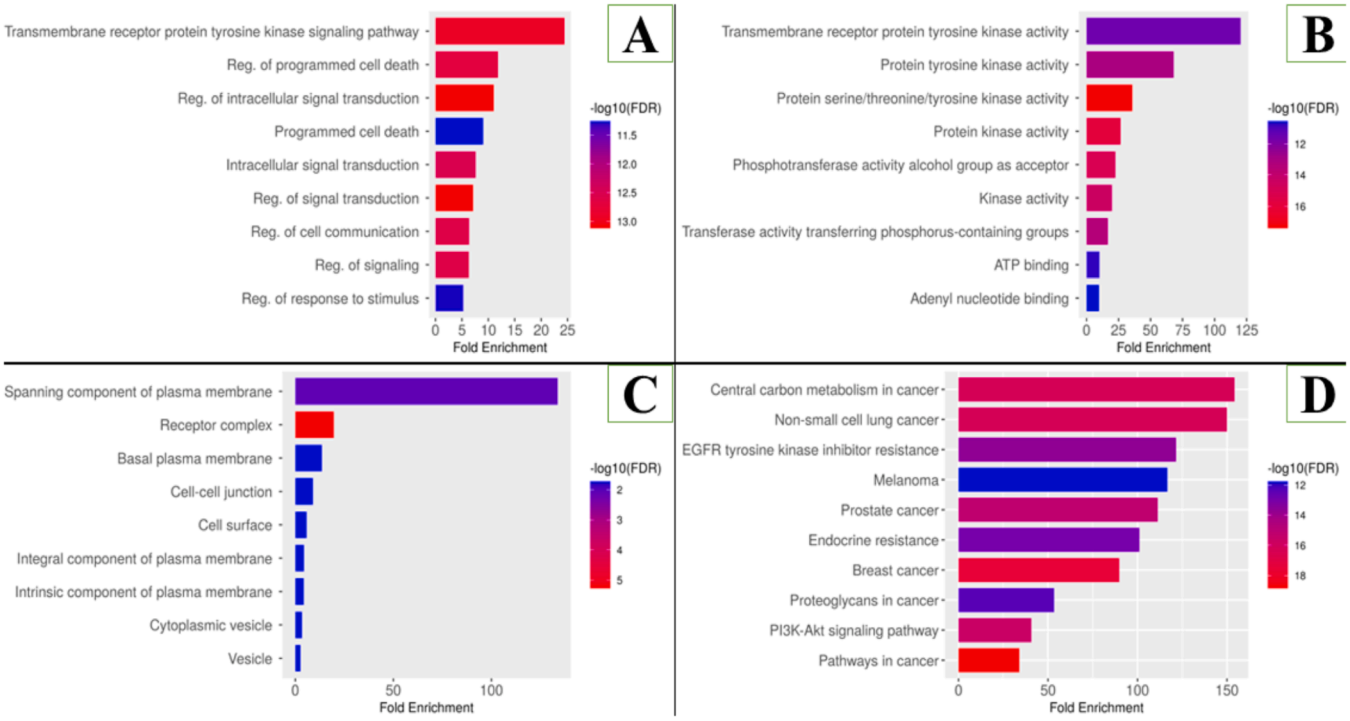

Fig. 3. Bar Plots representing the Enrichment analysis based on Fold Enrichment.

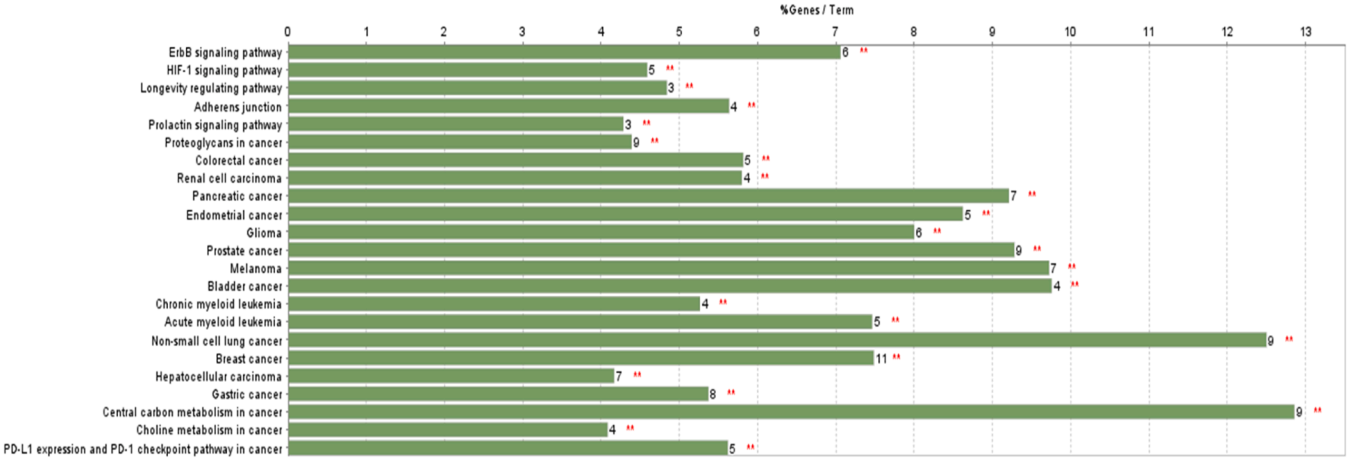

Fig. 4. Enrichment Pathway of GO Biological Process obtained from ClueGo Software.

drugs will be most active against breast cancer. The GO Biological process enrichment also proved that the query molecules act on the epidermal growth factor receptor signaling pathway, mammary gland epithelium development and cell proliferation, given in Fig. 7. Based on the obtained results, it merely showed that the compounds were most active against breast cancer. Even the results on the ShinyGO tool also showed that the query molecules act against the different pathways of breast cancer, the ClueGO clearly confirmed and explained the activity against breast cancer. The expression of both EGFR and HER2 has been proven to have an inverse correlation with the presence of estrogen receptors (ER), and it has also been demonstrated that EGFR/HER2 heterodimers have the ability to increase the metastatic potential of breast cancer cell lines. The high rate of EGFR overexpression that is associated with TNBC is one of the reasons why EGFR inhibitors are among the targeted therapies that are currently being investigated for the treatment of TNBC [69].

Protein sequence alignment

When exploring a protein sequence alignment, one of the initial and most impactful steps is to discern the highly conserved regions from those that exhibit lower conservation. We initially downloaded the Fasta sequence of retroviral protein PDB ID: 7BRO (Crystal structure of the nCoV main protease protein) and two other cancer proteins PDB ID: 3PPO (Crystal Structure of the Kinase domain of Human HER2), PBD ID: 5LX6 (Human PARP10 (ARTD10), catalytic fragment in complex with PARP inhibitor Veliparib), these three proteins Fasta sequence is compiled as a single sequence file. Based on the aligned sequence of three proteins: Cystine, Glycine, Proline, Alanine, Tyrosine, and Leucine are part of the conservative region. Focusing on the conserved region amino acids may result in less selectivity among the targets. Hence for selective inhibition, we have identified the semi-conserved region amino acids including Arginine, Asparagine, and Phenylalanine are crucial for biological activity. The phylogenetic tree sequence alignment is given in Fig. 8.

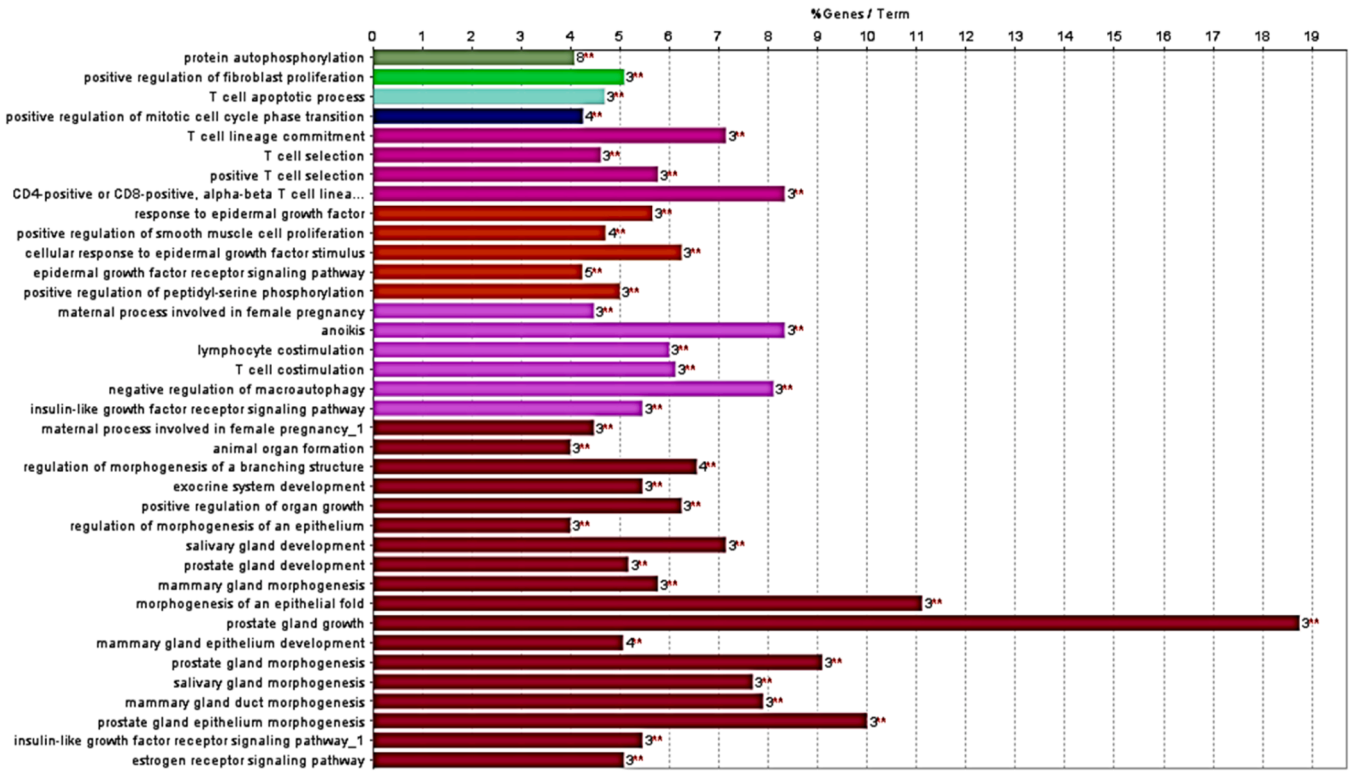

Fig. 5. KEGG enrichment pathway obtained from ClueGo software.

Molecular docking studies

It is a computational program that offers potential identification of all possible interactions between the ligand and the target active site. The chemical structures were elucidated by sketching and optimizing the repurposing of drug compounds. The approaches were furthered to rigid receptor docking in which the receptor is kept rigid, and the ligand can adopt various conformations and orientations to achieve optimal binding within the receptor's active site of HER2 and PARP proteins. Moreover, the MMFF94 force field parameters were needed to fit and execute in Autodock to make molecular simulations and structural studies more precise followed by the removal of water molecules and the co-crystallized ligands from the protein's active site. The selection of the active site is based mainly on the size of the active site and the interaction with the Co-crystallised residues. The results of the docking score of the compounds are shown, which gives an idea of the affinities of the ligand with the receptor, and the structures of the top two compounds are indicated in Fig. 9.

Each compound underwent ten conformations and was given an accurate binding score. As far the HER2 protein is concerned, among the 27 drug compounds, the top four compounds are Fostemsavir −8.17 Kcal/mol, Efavirenz −7.92 Kcal/mol, Doravirine −7.44 Kcal/mol, and Didanosine −7.11 Kcal/mol. The key residues responsible for the activity are ASN 850, ARG 849 and MET 801, the interpreted results are given in Table 3 along with the 2D and 3D ligand interaction diagrams in **Figure S1**. When it comes to the PARP protein the front runners are Efavirenz −8.08 Kcal/mol, Lopinavir −8.01 Kcal/mol, Fostemsavir −7.91 Kcal/mol and Elvitegravir −7.27 Kcal/mol, with regards to the residues TYR 919, PHE 909, and ASN 903, these key residue interactions correspond to the better binding affinity when compared with another study on PARP inhibitors [70]. **Figure S2** and Table 4 give detailed insights into the docking results of PARP protein. Taking these two protein targets into account, the drug compound Efavirenz belongs to a non-nucleoside reverse transcriptase inhibitor and Fostemsavir belongs to the class of HIV-1 gp120 inhibitor found to have a better chance against tumor suppression.

ADMET analysis

Pharmacokinetic and pharmacodynamic studies are essential for assessing a compound's drug-likeness. Even if a compound shows strong activity in experimental studies, it must satisfy all drug-likeness criteria to progress to clinical trials. In this study, the top two compounds—efavirenz and fostemsavir—were identified through docking studies. Although both compounds are proven drug candidates, their pharmacokinetic properties were further evaluated using the SWISSADME and Molinspiration tools. Efavirenz, with a molecular weight of 315.67 g/mol, 21 heavy atoms, 1 rotatable bond, 5 H-bond acceptors, and 1 H-bond donor, has zero Lipinski violations. In contrast, fostemsavir, with a molecular weight of 704.62 g/mol, 49 heavy atoms, 13 rotatable bonds, 15 H-bond acceptors, and 6 H-bond donors, has 3 Lipinski violations.

Molecular dynamics simulation

The research employed molecular dynamics simulations to assess the stability and interaction patterns within a complex. Specifically, dynamic simulations were conducted on the protein-ligand complexes of four chosen compounds. Analysis of these complexes was conducted utilizing metrics such as Root Mean Square Deviation, Root Mean Square Fluctuation, and examination of Protein-Ligand contacts. Notably, the 200 ns simulation of the complex yielded promising data. Trajectories were scrutinized using the simulation diagram interface of the Desmond suite. Supplementary materials include a video file showcasing the simulation trajectory.

Relative mean square deviation

Protein analysis

During the molecular simulation studies, the protein undergoes conformational changes when interacting with the ligand residues. Ensuring the stability of the complex is critical for subsequent analyses. Typically, deviations within the range of 1–3 Å are considered acceptable; deviations beyond this range indicate instability and failure to

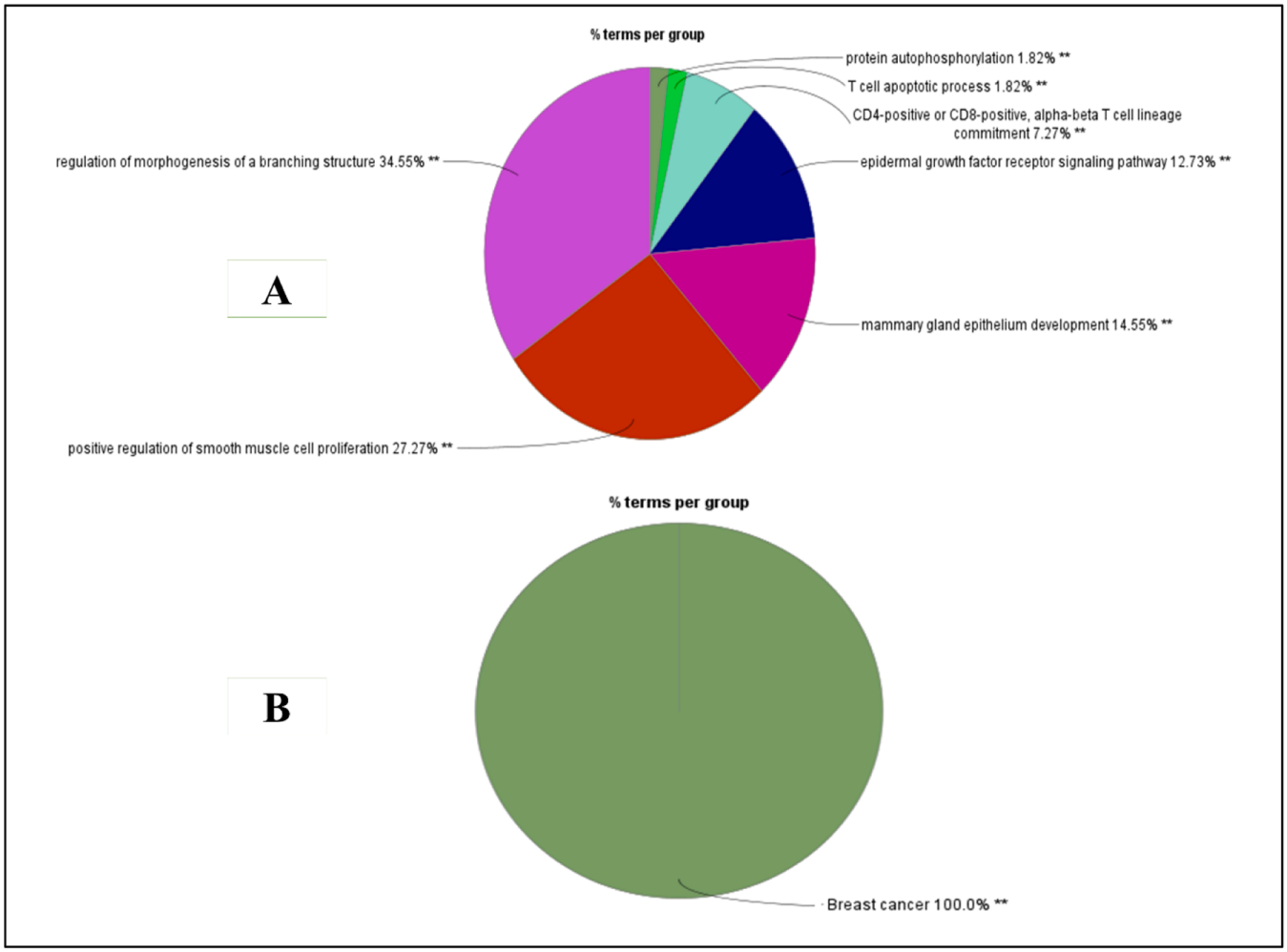

Fig. 6. Pie charts representing the GO biological process (A) and KEGG (B) Pathways obtained from ClueGO Software.

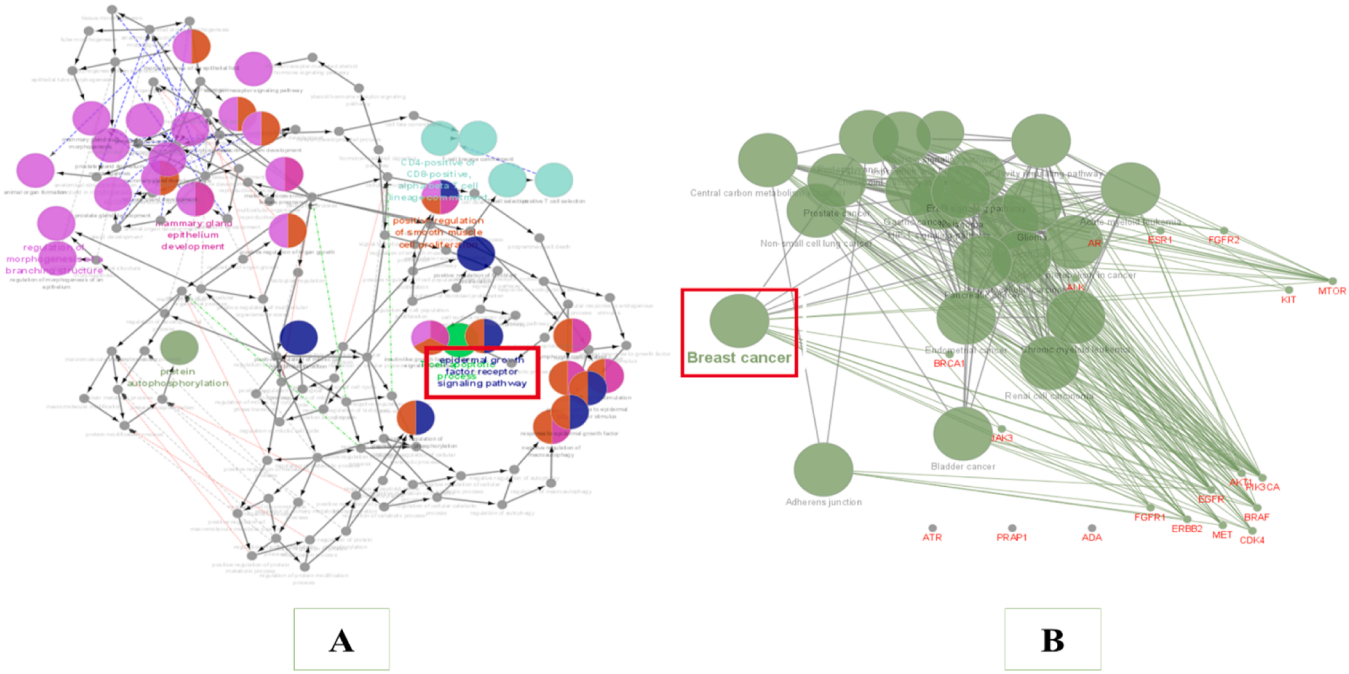

Fig. 7. Functional and Enrichment Pathway Analysis on ClueGO software.

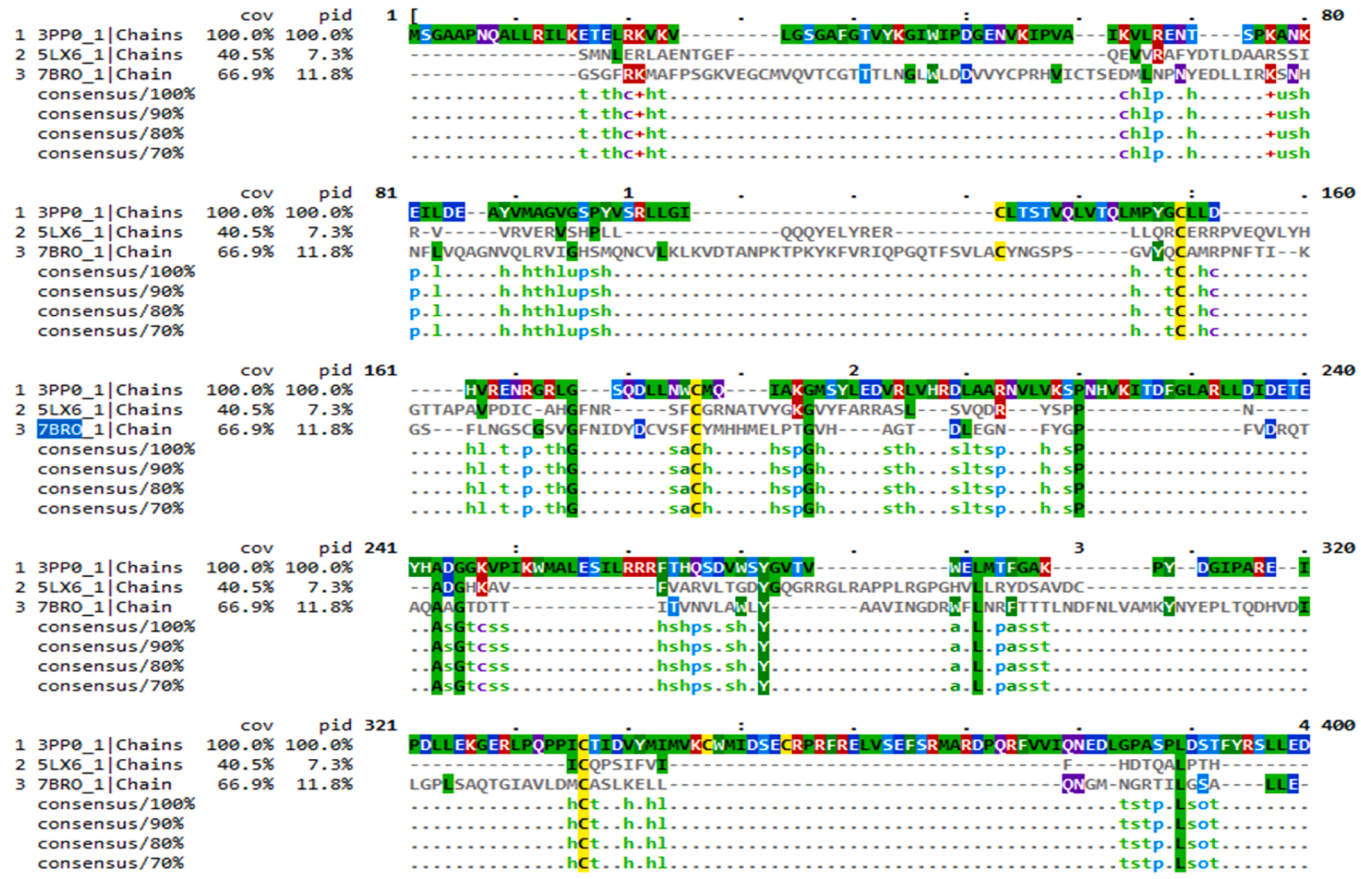

Fig. 8. An alignment of the HER2, PARP-1, and Protease proteins was generated using Clustal Omega. The figure displayed here is a modified representation of the Clustal Omega alignment of these three protein sequences.

reach equilibrium. In our study, the HER2 protein-ligand complexes involving Fostemsavir and Efavirenz demonstrated stability within these limits, with maximum deviations of 3.2 Å and 2.2 Å, respectively. The average RMSD of the protein backbone C-alpha was 1.8 Å, indicating stability throughout the simulation. Similarly, the Doravirine and Didanosine complexes showed maximum deviations of 4.0 Å and 2.7 Å, with average RMSDs of 2.2 Å, which also fall within acceptable boundaries. However, these complexes exhibited deviations during the simulation, suggesting lower effectiveness compared to Fostemsavir and Efavirenz, as shown in Fig. 10.

For the PARP protein-ligand complexes (Fig. 11), Efavirenz displayed excellent stability, with a maximum deviation of 2.4 Å and an average RMSD of 1.0 Å throughout the simulation. The Fostemsavir complex also showed strong stability, with a maximum deviation of 2.4 Å and an average RMSD of 1.2 Å, indicating good potential for inhibitory activity. Similar stability was observed for the Lopinavir and Elvitegravir complexes, with maximum RMSDs of 2.7 Å and 2.0 Å, respectively. Overall, Efavirenz and Fostemsavir demonstrated the most remarkable stability concerning C-alpha for both the HER2 and PARP receptor proteins.

Ligand analysis

In examining the ligand fit within protein complexes, we observed varying deviations during the 200 ns simulation period for HER2. Once the initial phase passed, the complex showed excellent stability for Efavirenz. For Fostemsavir, deviations occurred at regular intervals, but they remained within the acceptable range of 3.0 Å In contrast, the Doravirine and Didanosine complexes exhibited deviations of 4.8 Å and 2.7 Å, respectively, showing both positive and negative fluctuations. Fig. 10 provides further insight into these deviations.

Fostemsavir and Efavirenz stood out as exceptions, with a maximum RMSD of 4.0 Å, while the average deviation remained within 2.5 Å, indicating a high level of stability, particularly concerning ligand fit within the protein for both the HER2 and PARP receptors. In the case of the PARP receptor complex, Efavirenz and Lopinavir showed similar ligand-protein interactions, with a maximum RMSD of 4.8 Å and an average RMSD of 3.0 Å, demonstrating appreciable stability throughout the simulation. On the other hand, Fostemsavir and Elvitegravir complexes exhibited deviations of 5.4 Å and 13.5 Å, respectively. Notably, Efavirenz emerged as the most promising compound, with an average RMSD of 2.6 Å and a maximum RMSD of 4.8 Å, both within the acceptable range and showing minimal fluctuation. This complex maintained stability throughout the simulation period. Fig. 11 illustrates the RMSD of the protein-ligand complex, providing a graphical representation of its stability over the 200 ns simulation time.

Relative mean square fluctuation

Upon ligand binding to a protein, structural changes occur within the protein, influencing the Root Mean Square Fluctuation (RMSF) plot. This interaction can destabilize the protein structure, leading to increased fluctuations in the RMSF. Variations in hydrogen bonds, van der Waals forces, and electrostatic interactions between the protein and ligand contribute to this behavior. Additionally, ligand binding can enhance the overall flexibility of the protein structure, enabling it to adopt multiple conformations, thus increasing the RMSF values.

The RMSF analysis reveals uniform thermal motion along the protein chain, with mild fluctuations in helices and loops. Fluctuations exceeding 4.0 Å indicate strong hydrogen bond interactions. Terminal regions (N- and C-termini) exhibit more pronounced fluctuations

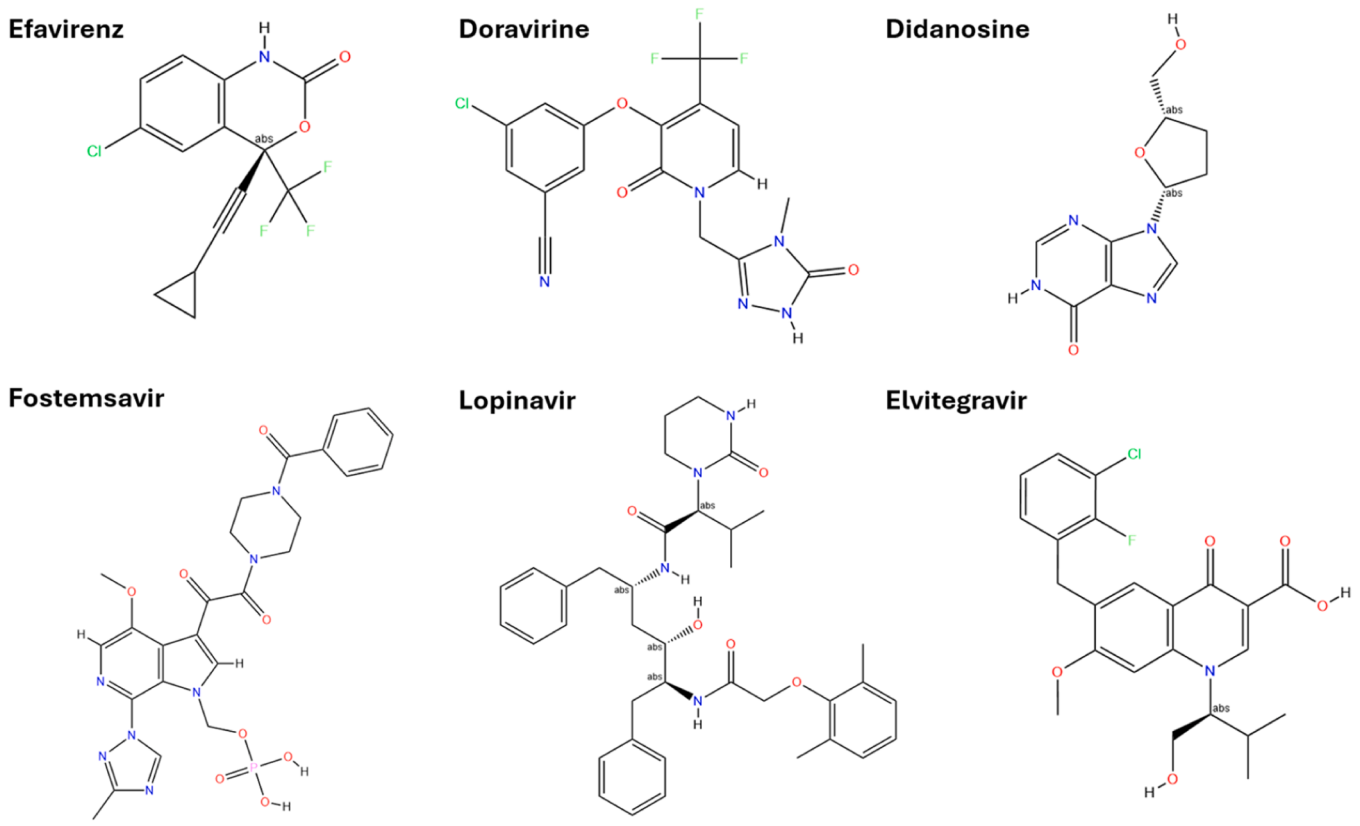

Fig. 9. Structures of the top compounds based on the docking results.

Table 3
Interpreted molecular docking results of drug compounds with HER2 receptor.

S. No	Drug	PubChem ID	Docking score	Key Residues
1	Fostemsavir	11,319,217	−8.17 Kcal/mol	ARG849,ASN850, SER728,ARG81
2	Efavirenz	64,139	−7.92 Kcal/mol	ASN850
3	Doravirine	58,460,047	−7.44 Kcal/mol	ASN850, ARG849
4	Didanosine	135,398,739	−7.11 Kcal/mol	MET801,CYS805, ASP808

Table 4
Interpreted molecular docking results of drug compounds with PARP receptor.

S. No	Drug	PubChem ID	Docking score	Key Residues
1	Efavirenz	64,139	−8.08 Kcal/mol	TYR919
2	Lopinavir	92,727	−8.01 Kcal/mol	PHE906,ARG931,GLY888
3	Fostemsavir	11,319,217	−7.91 Kcal/mol	HIS887,ASN910,TYR919, CYS907
4	Elvitegravir	5,277,135	−7.27 Kcal/mol	TYR919, ASN903,PHE906

compared to other segments. Regions with greater rigidity, such as helices and strands, show lower fluctuations, while loop regions, which are active for 80 % of the simulation, exhibit higher fluctuations. On average, the protein backbone shows an RMSF value of 2.5 Å For the HER2 protein, the average RMSF value for Efavirenz and Fostemsavir is 2.2 Å, while for Doravirine and Didanosine, the values are 2.7 Å and 2.2 Å, respectively. The fluctuation graphs, shown in Fig. 12, depict the fluctuations corresponding to the residue index for both compounds.

Regarding the RMSF analysis with the PARP receptor, Efavirenz demonstrated excellent fluctuation behavior, with an average fluctuation of <1.4 Å Fostemsavir, with an average fluctuation of 2.2 Å, showed promising results. Similar fluctuations were observed for Lopinavir and Elvitegravir, though the N- and C-terminal fluctuations were relatively smaller compared to Fostemsavir. Fig. 13 provides a detailed representation of the fluctuation data for the top four selected compounds with the PARP receptor.

Protein-ligand contact

The histogram graphic, generated from dynamics calculations, serves as a validation parameter for the docking results, elucidating the significant amino acids involved in biological activity. The complex interplay of hydrogen bonds ('H' bonds), hydrophobic contacts, water bridges, and ionic interactions is illustrated in the Figure. With the Amino acid residues binding in the X-axis and the interaction fraction on the Y-axis, the protein-ligand contact gives valuable information. Fig. 14 gives the data about the Protein-ligand contact of HER2 receptor protein, Efavirenz having the highest H bond fraction of 1.75 with MET801 and 0.5 fractions with ARG 849. For Fostemsavir 1.4 fraction of H bond with ARG 849, and similar fractions alongside water bridges with SER 728, ARG 863, With Doravirine ARG 849 with a maximum fraction of 1.0, Didanosine contact with protein has the fraction of 2.0 with MET 801. Fig. 15 gives the histogram graphic of protein-ligand contact of PARP receptor with selected four compounds, for Fostemsavir the maximum H bond fractions are with HIS 887, GLY 888, THR 890 and other important fractions includes TYR 919,TYR 932. Efavirenz showed similar fractions with PARP receptor as like that of HER2, with highest fraction of 1.75 with TYR 919, ASN 910 and many important residues, lopinavir shares similar fraction with Efavirenz, and Elvitegravir shows a maximum fraction of 1.0 with very few residues like ASP 896 and PHE

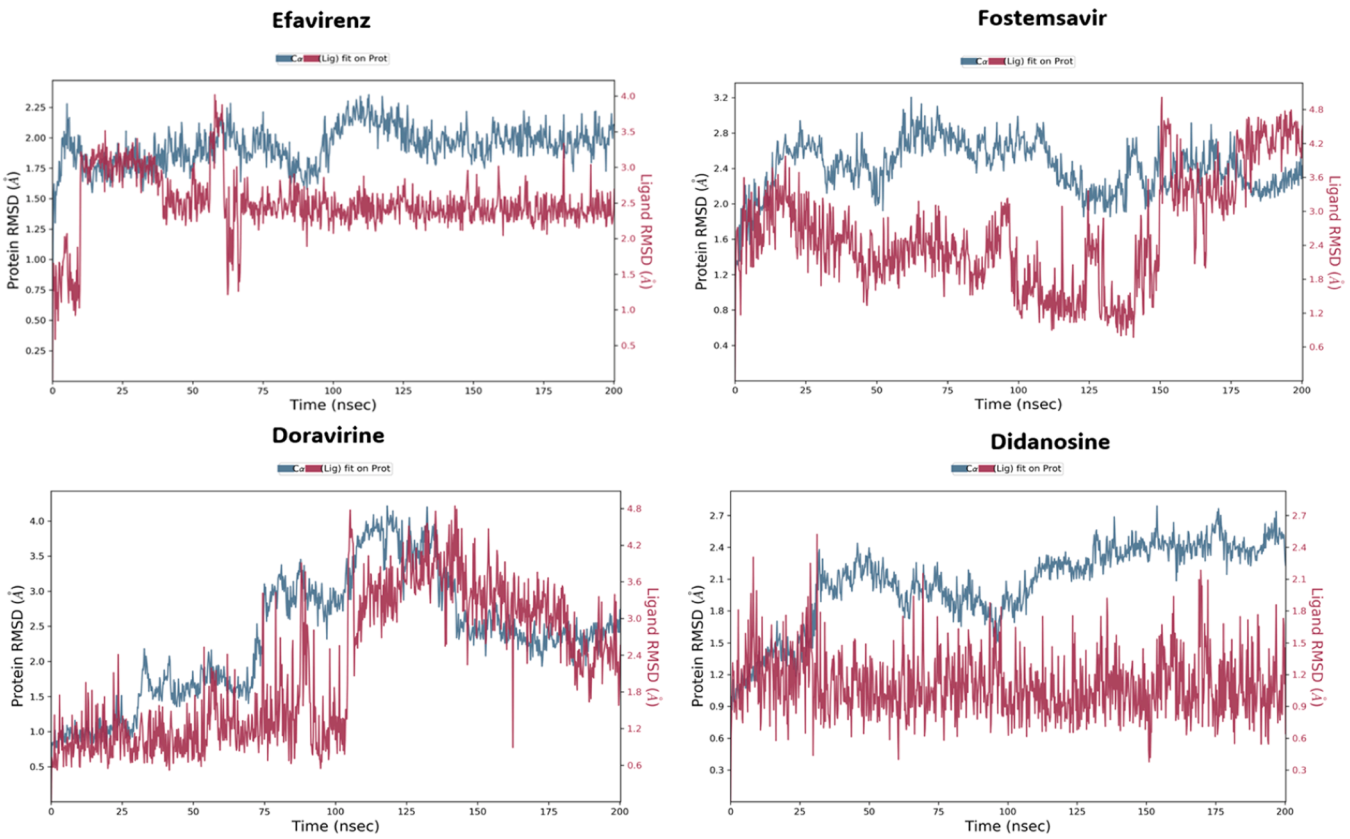

Fig. 10. Protein-ligand RMSD analysis of the top drug compounds with HER2 receptor 1) Efavirenz 2) Fostemsavir 3) Doravirine 4) Didanosine. (Blue – Protein, Red – Ligand).

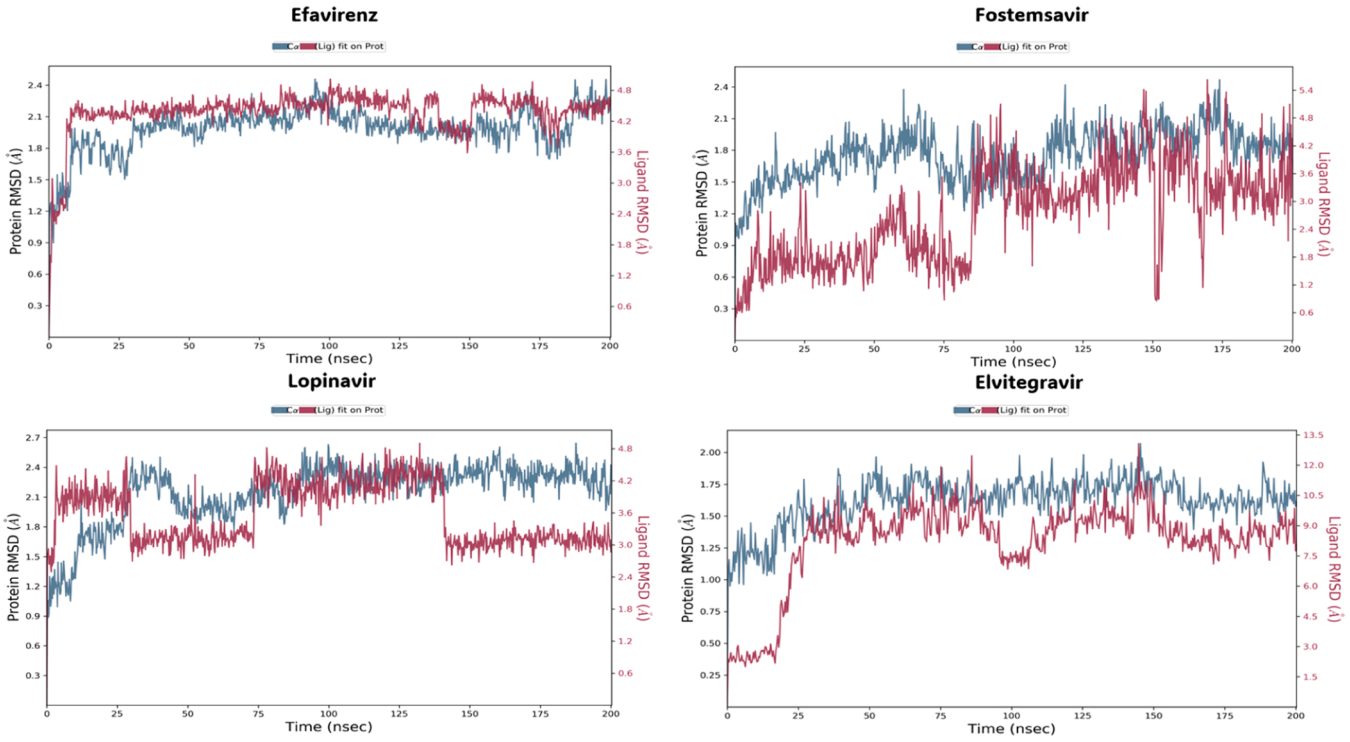

Fig. 11. Protein-ligand RMSD analysis of the top drug compounds with PARP receptor 1) Efavirenz 2) Fostemsavir 3) Lopinavir 4) Elvitegravir Blue – Protein, Red – Ligand).

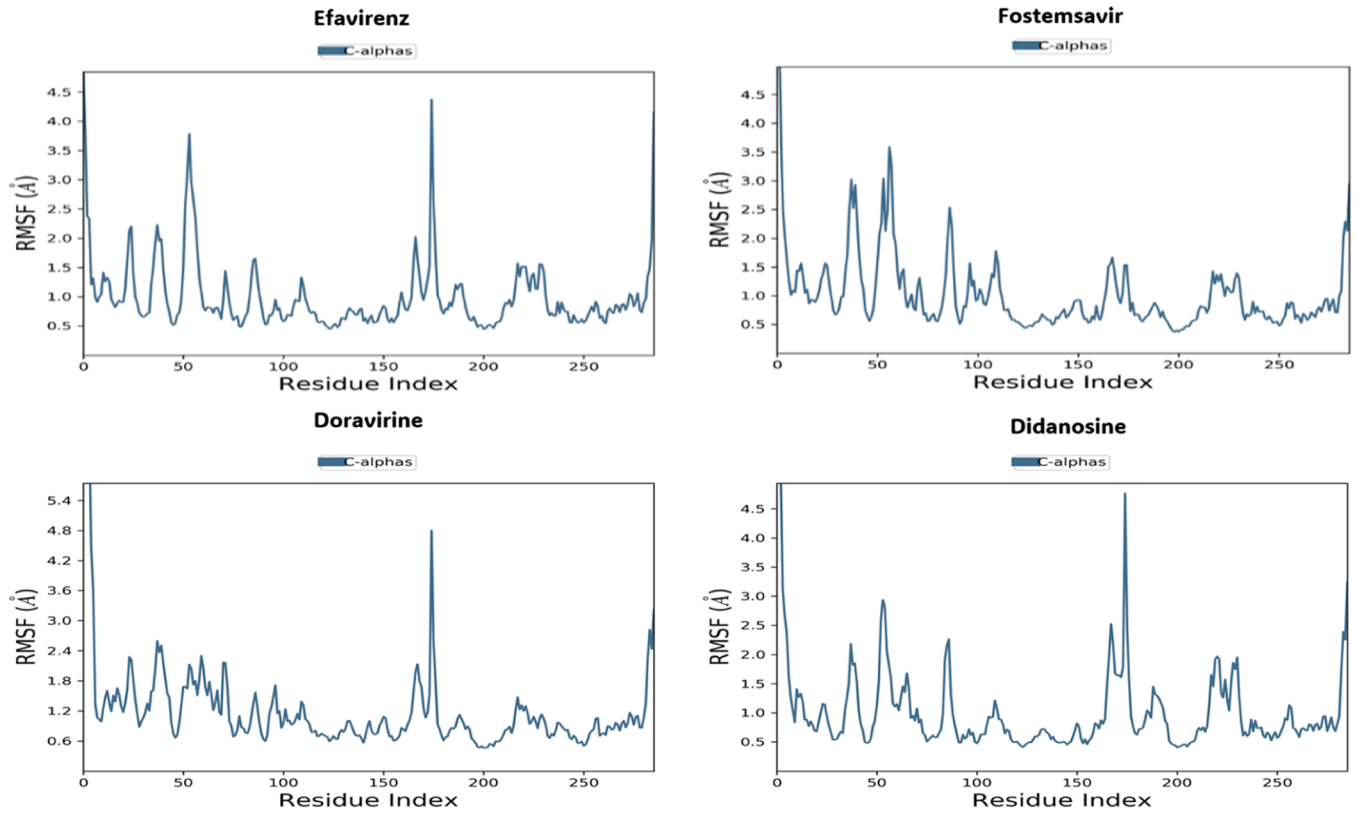

Fig. 12. Protein RMSF analysis of the top four drug compounds with HER2 receptor having residue index in X axis. 1) Efavirenz 2) Fostemsavir 3) Doravirine 4) Didanosine.

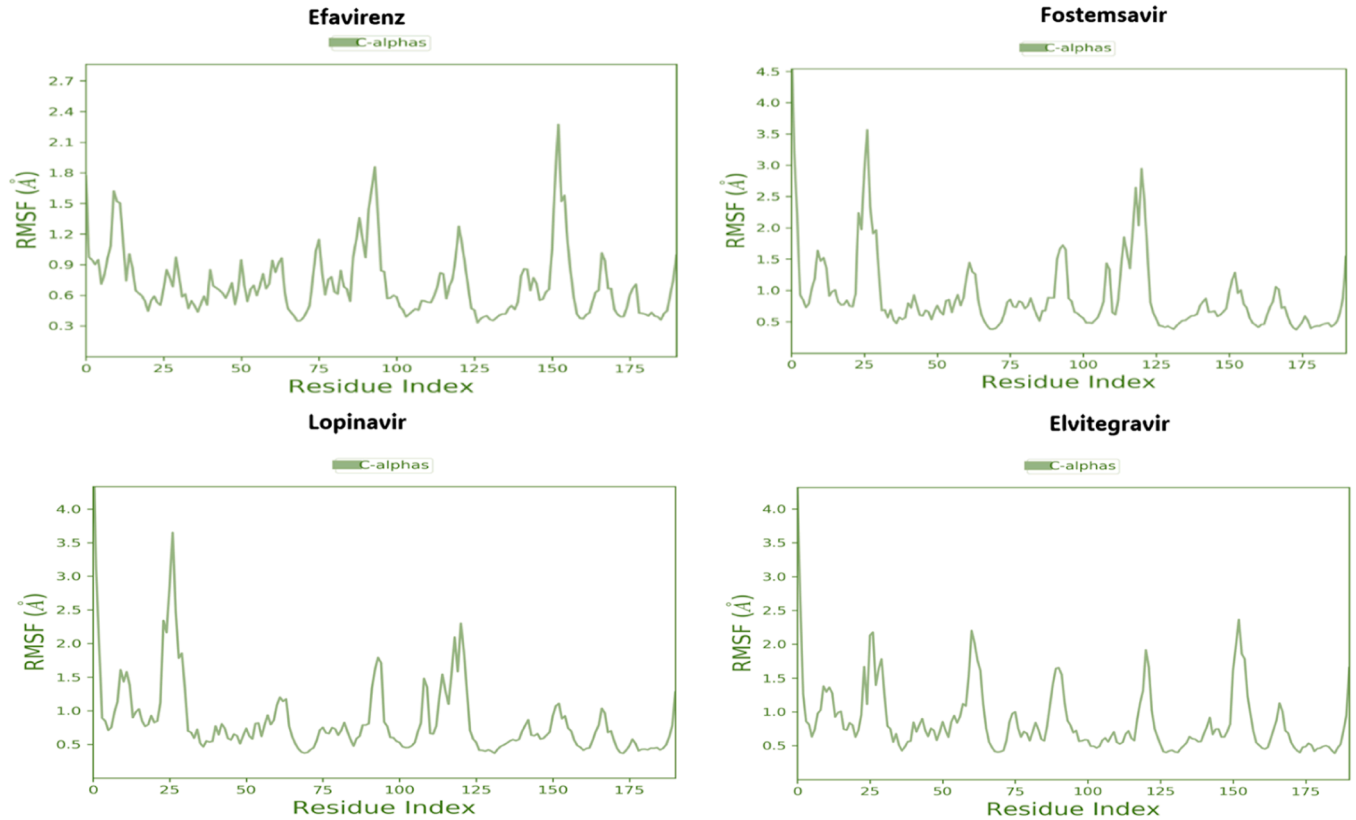

Fig. 13. Protein RMSF analysis of the top four drug compounds with PARP receptor having residue index in X axis. 1) Efavirenz 2) Fostemsavir 3) Lopinavir 4) Elvitegravir.

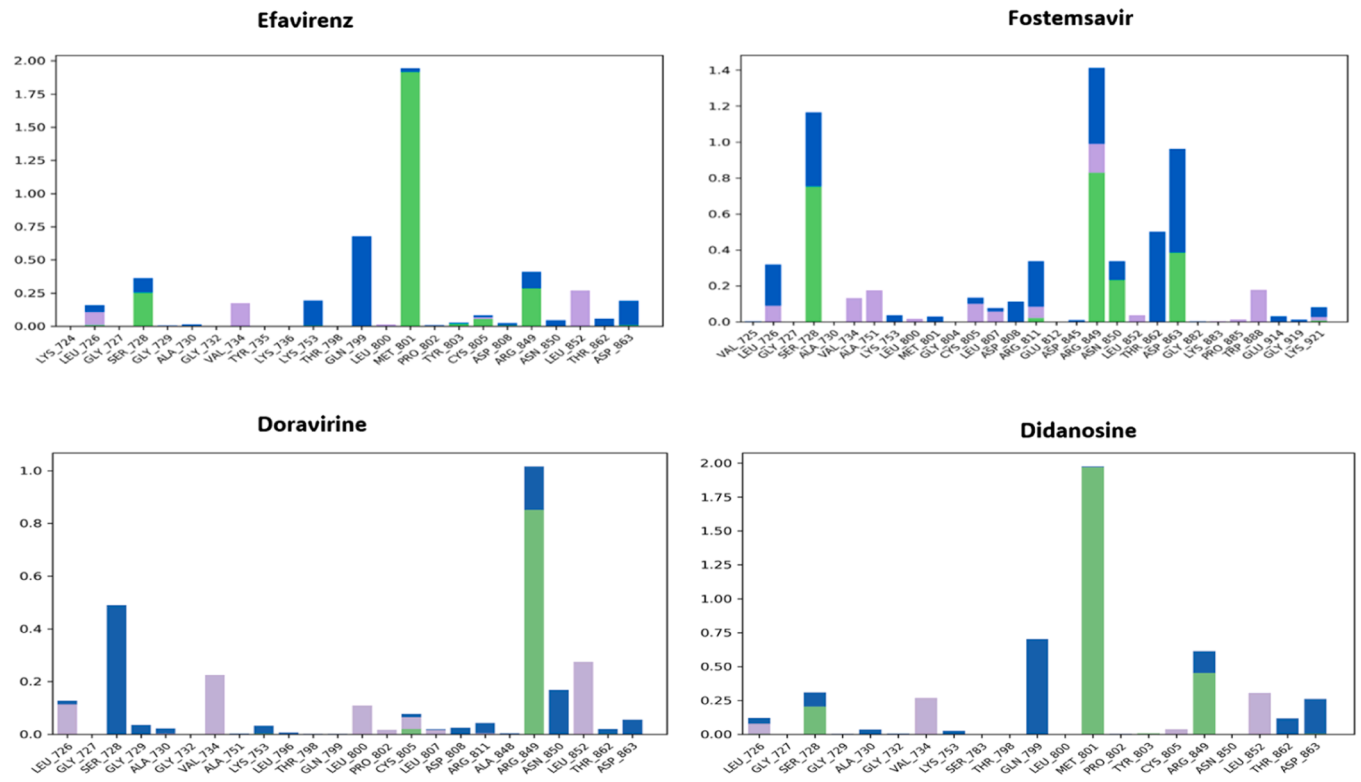

Fig. 14. Protein-ligand contact histogram of selected four compounds with HER2 receptor having Amino acid residues in X axis and Interaction fraction in Y axis.

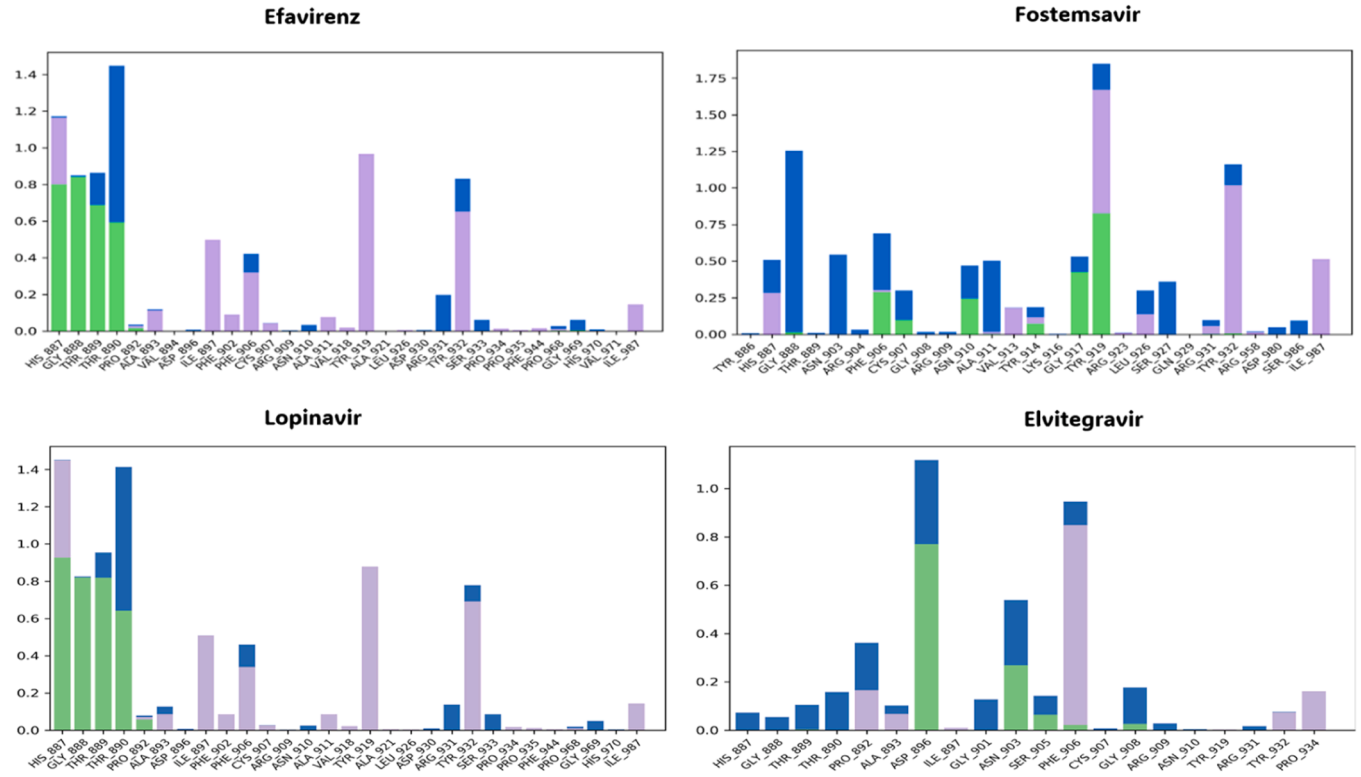

Fig. 15. Protein-ligand contact histogram of selected four compounds with PARP receptor having Amino acid residues in X axis and Interaction fraction in Y axis.

906.

Secondary structure elements

Maintaining the integrity of secondary structure elements holds paramount importance for the biological functionality of proteins.

Alterations in these structures, particularly in pivotal areas, have the potential to impact the protein's binding affinity, stability, and overall efficacy. Key secondary structure components such as α-helices and β-strands wield significant influence over the stability and functional capabilities of proteins. The interpreted value with the graph is given in **Supplementary Figure S3 and S4**, with its apoprotein RMSD and RMSF graphs are given in **Figure S5**.

Ligand properties

The molecular dynamics simulations of Efavirenz and Fostemsavir with HER2 and PARP reveal distinct insights into the stability and structural behavior of each complex over time, based on parameters such as radius of gyration (Rg), polar surface area (PSA), solvent-accessible surface area (SASA), and intramolecular hydrogen bonds (intraHB).The Rg values remained within a stable range, suggesting that both Efavirenz and Fostemsavir form moderately stable complexes with HER2 and PARP. However, Efavirenz-HER2 and Efavirenz-PARP showed slightly more consistent Rg values than their Fostemsavir counterparts, which may imply that Efavirenz has a more stabilizing effect on these proteins. Regarding the PSA values, which reflect the accessible polar surface areas, showed slight variations across all complexes. The Efavirenz complexes with HER2 and PARP presented consistent PSA values, indicating a stable interaction with limited exposure of polar regions. In contrast, Fostemsavir complexes showed slightly higher PSA fluctuations, especially with PARP, suggesting variations in the exposure of polar groups. The Efavirenz complexes demonstrated observable intraHB fluctuations, indicative of some degree of structural stability and flexibility. However, no intramolecular hydrogen bonds were detected for either Fostemsavir-HER2 or Fostemsavir-PARP complexes, which may suggest a lack of stabilizing intramolecular interactions. The absence of intraHB in Fostemsavir complexes could be linked to its different binding mode or a conformational instability that might impact its effectiveness in a biological setting. These findings in **Figure S6** suggest that Efavirenz may have a more stable binding interaction with these targets compared to Fostemsavir, which may require optimization to enhance its stability and efficacy.

Molecular mechanism generalized born surface area

For the determination of binding free energy between both HER2 and PARP receptor proteins and drug complex, the Prime MM-GBSA technique within molecular mechanics generalized Born surface area (MM-GBSA) was used. In the current work, the Schrodinger suite was used along with the OPLS-2005 force field and its Prime module in the calculation of binding free energies of the receptor-ligand complexes. A general consensus in the scientific literature is that ligands that reach more negative binding energy (ΔG) shed better conformational restriction and stronger non-covalent bonds within protein-ligand complexes. Strong interaction of our ligand with the active site of the receptor protein indicates strongly associating non-covalent interactions that are part of the protein-ligand complex in the system. This stability is attributed by crucial active site residues like ARG 849, ASN 850 and MET 801 for HER2 receptor protein, whereas in the case of PARP protein TYR 919, PHE 906 and ASN 910. Particularly, Efavirenz and Fostemsavir exhibits a high binding free energy of −45.35 kcal/mol and −30.36 kcal/mol respectively for HER2 and with the PARP receptor protein Efavirenz showed the binding free energy of −46.45 kcal/mol and −35.28 Kcal/mol. Fostemsavir, showcasing stability across multiple criteria, results are interpreted and tabulated in Table 5. Visual representations in both 2D and 3D of the drug receptor complex of Efavirenz and Fostemsavir with both the proteins HER2 and PARP at various time intervals (50 ns, 100 ns, 150 ns, and 200 ns) of molecular simulation are depicted in **Figure S7** and **Figure S8** respectively.

Table 5
Binding free energy (Molecular Mechanics Generalized Born Surface Area) of the top two selected compounds with HER2 and PARP receptors.

Drug Complex	ΔE vdw (Kcal/mol)	ΔG H bond (Kcal/mol)	ΔG mmgbsa (Kcal/mol)	ΔG (binding) (Kcal/mol)
Efavirenz-HER2	−45.356	−2.5475	−59.822	−68.106
Fostemsavir-HER2	−30.365	−0.3445	−25.901	−27.996
Efavirenz-PARP	−46.452	−2.2436	−72.070	−83.691
Fostemsavir-PARP	−35.289	−0.6622	−46.632	−49.072

Normal mode analysis

Based on the results of molecular dynamics and free energy calculations, the efavirenz-HER2 and efavirenz-PARP complexes were taken for normal mode analysis to calculate the entropy of the system. In molecular systems, vibrational entropy is related to the number of accessible vibrational states, and it can reflect the conformational flexibility of the complex. Using the formula given in the methodology section the vibrational entropy of the system is calculated from the selected lower frequency modes 7–20, for the Efavirenz-HER2 complex the entropy was found to be 9.774 kcal mol^{-1} K^{-1} and for the Efavirenz-PARP complex it was found to be −10.418 kcal mol^{-1} K^{-1}, these values suggest moderate flexibility in the efavirenz complexes, which could influence its binding behavior and thermodynamics.

Principal component analysis

To investigate the collective movements within the complexes, Principal Component Analysis (PCA) was performed, based on the dynamics and free energy calculation, Efavirenz-HER2 and Efavirenz-PARP complexes are taken for PCA calculation. The dominant modes of motion, represented by the first few eigenvectors (EVs), play a critical role in defining the overall dynamics of protein molecules. The results revealed lower overall flexibility in both EVs, as shown by the time evolution of PCA, suggesting high stability of the complexes. Fig. 16 illustrates that the Efavirenz-HER2 and Efavirenz-PARP complexes occupied overlapping conformational spaces, encompassing most of their collective movements. The limited range of motions observed in these systems indicates that Efavirenz binding did not significantly perturb the target proteins' conformations or dynamics, further confirming the stability of the complexes.

Conclusion

Exploring the various techniques used in the novel drug discovery process, optimizing it, and applying it in the drug repurposing strategy is very fruitful. We carefully curated a series of 76 drug molecules of various inhibitors under the class of anti-retroviral, and the molecules are further screened for their potential against cancer targets like HER2 and PARP-1 proteins. Before analyzing the drug molecules' suitability with the cancer targets, we have studied the protein sequence alignment of the cancer and anti-retroviral proteins, and we have found the crucial role of semi-conserved region residues like ARG, ASP, and PHE. Molecular docking studies are carried out to correlate the results of sequencing and to find the drug-receptor interaction, based on the results, we have discovered that Fostemsavir −8.17 Kcal/mol, Efavirenz −7.92 Kcal/mol, Doravirine −7.44 Kcal/mol, and Didanosine −7.11 Kcal/mol are the best compounds in HER2 receptor, whereas for PARP-1, Efavirenz −8.08 Kcal/mol, Lopinavir −8.01 Kcal/mol, Fostemsavir −7.91 Kcal/mol, and Elvitegravir −7.27 Kcal/mol found to be the best. Then these four drugs were taken for further dynamic simulation studies, where the results showed that the Efavirenz drug acting on both

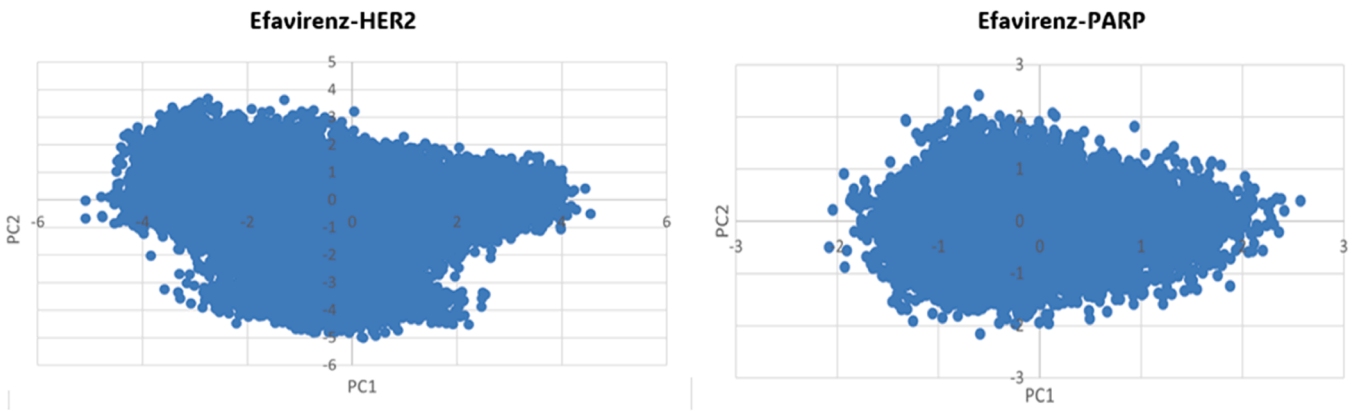

Fig. 16. Principal component analysis 2D projection plot shows the conformation sampling of complexes Efavirenz-HER2 and Efavirenz-PARP.

the targets had excellent stability over the complex, binding free energy calculation shedding light on the biological activity of this drug molecules as a potential anticancer agent. Elucidating the mechanism of action of Efavirenz against HER2 and PARP-1 opens up new opportunities for translating these findings into innovative therapies. These therapies have the potential to reduce the burden of cancer and enhance the quality of life for those affected.

Funding

This research did not receive any specific grant from funding agencies in the public, commercial, or not-for-profit sectors.

CRediT authorship contribution statement

Uma Maheshwari Mugundan: Methodology, Investigation, Formal analysis, Data curation, Conceptualization. **Praveen Sekar:** Writing – original draft, Software, Methodology. **Rajanandh Muhasaparur Ganesan:** Writing – review & editing, Writing – original draft, Validation, Supervision, Resources, Project administration.

Declaration of competing interest

The authors declare that they have no known competing financial interests or personal relationships that could have appeared to influence the work reported in this paper.

Acknowledgments

We thank the Management of SRM College of Pharmacy, and SRM Institute of Science and Technology for their constant support and encouragement.

Supplementary materials

Supplementary material associated with this article can be found, in the online version, at doi:10.1016/j.chphi.2024.100812.

Data availability

I have attached the research data availability statement

References

[1] Global Breast Cancer Initiative, Breast cancer, (2024). https://www.who.int/news-room/fact-sheets/detail/breast-cancer (accessed May 23, 2024).
[2] K. Sathishkumar, J. Sankarapillai, A. Mathew, R.A. Nair, N. Gangane, S. Khuraijam, D. Barmon, S. Pandya, G. Majumdar, V. Deshmane, E. Zomawia, T.W. Bhutia, K. Jerang, P.S. George, S. Maliye, R. Laishram, G. Das, A. Shah, S. Debbarma, S. Koyande, L. Pachuau, A. Sherpa, G. Jongkey, M. Chaturvedi, P. Das, S. Santhappan, P. Mathur, Breast cancer survival in India across 11 geographic areas under the National Cancer Registry Programme, Cancer 130 (2024) 1816–1825, https://doi.org/10.1002/cncr.35188.
[3] M. Porteous, D. Stirling, Breast Cancer. Brenner's Encyclopedia of Genetics, Elsevier, 2013, pp. 387–390, https://doi.org/10.1016/B978-0-12-374984-0.00173-X.
[4] Y.-S. Sun, Z. Zhao, Z.-N. Yang, F. Xu, H.-J. Lu, Z.-Y. Zhu, W. Shi, J. Jiang, P.-P. Yao, H.-P. Zhu, Risk factors and preventions of breast cancer, Int. J. Biol. Sci. 13 (2017) 1387–1397, https://doi.org/10.7150/ijbs.21635.
[5] C.I. Li, D.J. Uribe, J.R. Daling, Clinical characteristics of different histologic types of breast cancer, Br. J. Cancer 93 (2005) 1046–1052, https://doi.org/10.1038/sj.bjc.6602787.
[6] A.C. Wolff, S.M. Domchek, N.E. Davidson, V. Sacchini, B. McCormick, Cancer of the breast. Abeloff's Clinical Oncology, Elsevier, 2014, pp. 1630–1692, https://doi.org/10.1016/B978-1-4557-2865-7.00091-6, e9.
[7] Z. Mitri, T. Constantine, R. O'Regan, The HER2 receptor in breast cancer: pathophysiology, clinical use, and new advances in therapy, Chemother Res. Pract. 2012 (2012) 1–7, https://doi.org/10.1155/2012/743193.
[8] K. Won, C. Spruck, Triplenegative breast cancer therapy: current and future perspectives (Review), Int. J. Oncol. 57 (2020) 1245–1261, https://doi.org/10.3892/ijo.2020.5135.
[9] D.D. Singh, A. Parveen, D.K. Yadav, Role of PARP in TNBC: mechanism of inhibition, clinical applications, and resistance, Biomedicines 9 (2021) 1512, https://doi.org/10.3390/biomedicines9111512.
[10] T.C. de Ruijter, J. Veeck, J.P.J. de Hoon, M. van Engeland, V.C. Tjan-Heijnen, Characteristics of triple-negative breast cancer, J. Cancer Res. Clin. Oncol. 137 (2011) 183–192, https://doi.org/10.1007/s00432-010-0957-x.
[11] E.A. Rakha, M.E. El-Sayed, A.R. Green, A.H.S. Lee, J.F. Robertson, I.O. Ellis, Prognostic markers in triple-negative breast cancer, Cancer 109 (2007) 25–32, https://doi.org/10.1002/cncr.22381.
[12] R. Patnala, S.-H. Lee, J.E. Dahlstrom, S. Ohms, L. Chen, S.T. Dheen, D. Rangasamy, Inhibition of LINE-1 retrotransposon-encoded reverse transcriptase modulates the expression of cell differentiation genes in breast cancer cells, Breast Cancer Res. Treat. 143 (2014) 239–253, https://doi.org/10.1007/s10549-013-2812-7.
[13] I. Faraoni, G. Graziani, Role of BRCA mutations in cancer treatment with Poly (ADP-ribose) polymerase (PARP) inhibitors, Cancers (Basel) 10 (2018) 487, https://doi.org/10.3390/cancers10120487.
[14] R.U. Hernández-Ramírez, M.S. Shiels, R. Dubrow, E.A. Engels, Cancer risk in HIV-infected people in the USA from 1996 to 2012: a population-based, registry-linkage study, Lancet HIV 4 (2017) e495–e504, https://doi.org/10.1016/S2352-3018(17)30125-X.
[15] R.U. Hernández-Ramírez, M.S. Shiels, R. Dubrow, E.A. Engels, Cancer risk in HIV-infected people in the USA from 1996 to 2012: a population-based, registry-linkage study, Lancet HIV 4 (2017) e495–e504, https://doi.org/10.1016/S2352-3018(17)30125-X.
[16] N. Borcherding, Y. Jethava, P. Vikas, Repurposing anti-cancer drugs for COVID-19 treatment, Drug. Des. Devel. Ther. 14 (2020) 5045–5058, https://doi.org/10.2147/DDDT.S282252.
[17] F. Cheng, W. Lu, C. Liu, J. Fang, Y. Hou, D.E. Handy, R. Wang, Y. Zhao, Y. Yang, J. Huang, D.E. Hill, M. Vidal, C. Eng, J. Loscalzo, A genome-wide positioning systems network algorithm for in silico drug repurposing, Nat. Commun. 10 (2019) 3476, https://doi.org/10.1038/s41467-019-10744-6.
[18] A. Kumar, E. Rathi, S.G. Kini, Drug repurposing approach for the identification and designing of potential E6 inhibitors against cervical cancer: an in silico investigation, Struct. Chem. 31 (2020) 141–153, https://doi.org/10.1007/s11224-019-01378-x.
[19] P. Polamreddy, N. Gattu, The drug repurposing landscape from 2012 to 2017: evolution, challenges, and possible solutions, Drug. Discov. Today 24 (2019) 789–795, https://doi.org/10.1016/j.drudis.2018.11.022.
[20] H.S. GNS, S. GR, M. Murahari, M. Krishnamurthy, An update on drug repurposing: *re*-written saga of the drug's fate, Biomed. Pharmacotherapy 110 (2019) 700–716, https://doi.org/10.1016/j.biopha.2018.11.127.

[21] S. Priyankha, S. Polk, R. Thilagavathi, M. Prakash, M.K. Kathiravan, S. Lakshmana Prabhu, I. Brunozi de Oliveira, C. Selvam, The virtual screening of compounds from the ZINC database against PARP-1 in triple-negative breast cancer, Chem. Select 9 (2024), https://doi.org/10.1002/slct.202304729.

[22] P. Sekar, S. Arivanantham, P. Jaishankar, N. Sundhararajan, Y. Nagalingam, S. K. Raju, Graph theoretical analysis, pharmacoinformatics and molecular docking investigation of chalcone-schiff base hybrids as cyclin-dependent kinase inhibitors, Res. Pharm. (2024), https://doi.org/10.25081/rip.2024.v14.8801.

[23] C. Zhang, Y. Liao, L. Liu, Y. Sun, S. Lin, J. Lan, H. Mao, H. Chen, Y. Zhao, A network pharmacology approach to investigate the active compounds and mechanisms of musk for ischemic stroke, Evidence-Based Complem. Altern. Med. 2020 (2020), https://doi.org/10.1155/2020/4063180.

[24] P. Shannon, A. Markiel, O. Ozier, N.S. Baliga, J.T. Wang, D. Ramage, N. Amin, B. Schwikowski, T. Ideker, Cytoscape: a software environment for integrated models of biomolecular interaction networks, Genome Res. 13 (2003) 2498–2504, https://doi.org/10.1101/gr.1239303.

[25] T. Wang, Y. Feng, H. Wang, G. Huo, Y. Cai, L. Wang, K. Yuan, G. Huang, The mechanisms of sijunzi decoction in the treatment of chronic gastritis revealed by network pharmacology, Evidence-Based Complem. Altern. Med. 2020 (2020), https://doi.org/10.1155/2020/8850259.

[26] F. Wang, C.-L. Mo, M. Lu, X.-L. Deng, J.-Y. Luo, Network pharmacology to explore the mechanism of traditional Chinese medicine in the treatment of ground glass nodules, J. Thorac. Dis. 16 (2024) 2745–2756, https://doi.org/10.21037/jtd-23-1492.

[27] Y. Lu, J. Bi, F. Li, G. Wang, J. Zhu, J. Jin, Y. Liu, Differential gene analysis of trastuzumab in breast cancer based on network pharmacology and medical images, Front Physiol. 13 (2022), https://doi.org/10.3389/fphys.2022.942049.

[28] X. Ma, C. Hao, M. Yu, Z. Zhang, J. Huang, W. Yang, Investigating the molecular mechanism of quercetin protecting against podocyte injury to attenuate diabetic nephropathy through network pharmacology, microarraydata analysis, and molecular docking, Evidence-Based Complem. Altern. Med. 2022 (2022) 1–13, https://doi.org/10.1155/2022/7291434.

[29] M.Y. Sofi, A. Shafi, K.Z. Masoodi, Multiple sequence alignment. Bioinformatics For Everyone, Elsevier, 2022, pp. 47–53, https://doi.org/10.1016/B978-0-323-91128-3.00011-2.

[30] S.F. Altschul, W. Gish, W. Miller, E.W. Myers, D.J. Lipman, Basic local alignment search tool, J. Mol. Biol. 215 (1990) 403–410, https://doi.org/10.1016/S0022-2836(05)80360-2.

[31] S. McGinnis, T.L. Madden, BLAST: at the core of a powerful and diverse set of sequence analysis tools, Nucleic. Acids. Res. 32 (2004) W20–W25, https://doi.org/10.1093/nar/gkh435.

[32] N. Arumugam, A.I. Almansour, R.S. Kumar, V. Siva Krishna, D. Sriram, N. Dege, Stereoselective synthesis and discovery of novel spirooxindolopyrrolidine engrafted indandione heterocyclic hybrids as antimycobacterial agents, Bioorg. Chem. 110 (2021) 104798, https://doi.org/10.1016/j.bioorg.2021.104798.

[33] I. Sayer, N. Dege, H. Ghalla, A. Moliterni, H. Naïli, Crystal structure, DFT studies and thermal characterization of new luminescent stannate (IV) based inorganic-organic hybrid compound, J. Mol. Struct. 1224 (2021) 129266, https://doi.org/10.1016/j.molstruc.2020.129266.

[34] A. Bulut, O.Z. Yesilel, N. Dege, H. Icbudak, H. Olmez, O. Buyukgungor, Dinicotinamidium squarate, Acta. Crystallogr. C 59 (2003) o727–o729, https://doi.org/10.1107/S0108270103025903.

[35] S. Genç, N. Dege, A. Çetin, A. Cansız, M. Şekerci, M. Dinçer, 3-(2-Hydroxyphenyl)-4-phenyl-1 *H* -1,2,4-triazole-5(4 *H*)-thione, Acta. Crystallogr. Sect. E Struct. Rep. Online 60 (2004) o1580–o1582, https://doi.org/10.1107/S1600536804020367.

[36] F. Bracht, R.B. de Alencastro, Dynamical study, hydrogen bond analysis, and constant pH simulations of the beta carbonic anhydrase of *Methanobacterium thermoautotrophicum*, J. Biomol. Struct. Dyn. 34 (2016) 259–271, https://doi.org/10.1080/07391102.2015.1025100.

[37] X.-Y. Meng, H.-X. Zhang, M. Mezei, M. Cui, Molecular docking: a powerful approach for structure-based drug discovery, Current. Comput. Aided-Drug Design 7 (2011) 146–157, https://doi.org/10.2174/157340911795677602.

[38] N. Dege, Ö. Tamer, M. Şimşek, D. Avcı, M. Yaman, A. Başoğlu, Y. Atalay, Experimental and theoretical approaches on structural, spectroscopic (FT-IR and UV–Vis), nonlinear optical, and molecular docking analyses for Zn (II) and Cu (II) complexes of 6-chloropyridine-2-carboxylic acid, Appl. Organomet. Chem. 36 (2022), https://doi.org/10.1002/aoc.6678.

[39] E. Alaman, A.A. Ağar, M.N. Tahir, M. Ashfaq, E.B. Poyraz, N. Dege, Synthesis, structural, spectroscopic, hirshfeld surface analysis and computational study of copper complex containing salicylaldimine ligands, J. Struct. Chem. 64 (2023) 1314–1328, https://doi.org/10.1134/S0022476623070156.

[40] D. Tatlidil, M.A. Raza, N. Dege, A.A. Agar, U. Farwa, S.U. Rehman, Therapeutical potential of imines; synthesis, single crystal structure, computational, molecular modeling, and ADMET evaluation, ACS Omega 7 (2022) 10568–10579, https://doi.org/10.1021/acsomega.2c00102.

[41] N. Dege, Ö. Tamer, M. Şimşek, D. Avcı, M. Yaman, A. Başoğlu, Y. Atalay, Experimental and theoretical approaches on structural, spectroscopic (FT-IR and UV–Vis), nonlinear optical, and molecular docking analyses for Zn (II) and Cu (II) complexes of 6-chloropyridine-2-carboxylic acid, Appl. Organomet. Chem. 36 (2022), https://doi.org/10.1002/aoc.6678.

[42] M. Kurbanova, M. Ashfaq, M.N. Tahir, A. Maharramov, N. Dege, A. Koroglu, Synthesis, crystal structure, supramolecular assembly exploration by hirshfeld surface analysis and computational study Of 6-Bromo-2-Oxo- 2h-Chromene-3-Carbonitrile (BOCC), J. Struct. Chem. 64 (2023) 302–313, https://doi.org/10.1134/S0022476623020142.

[43] M.A. Raza, U. Farwa, M. Danish, S. Ozturk, A.A. Aagar, N. Dege, S.U. Rehman, A. G. Al-Sehemi, Computational modeling of imines based anti-oxidant and anti-esterases compounds: synthesis, single crystal and In-vitro assessment, Comput. Biol. Chem. 104 (2023) 107880, https://doi.org/10.1016/j.compbiolchem.2023.107880.

[44] S. Şahin, N. Dege, A newly synthesized small molecule: the evaluation against Alzheimer's Disease by in silico drug design and computational structure analysis methods, J. Mol. Struct. 1236 (2021) 130337, https://doi.org/10.1016/j.molstruc.2021.130337.

[45] S. Kansız, M. Azam, T. Basılı, S. Meral, F.A. Aktaş, S. Yeşilbağ, K. Min, A.A. Ağar, N. Dege, Synthesis, structural studies, Hirshfeld surface analysis, and molecular docking studies of a thiophene-based Schiff base compound, J. Mol. Struct. 1265 (2022) 133477, https://doi.org/10.1016/j.molstruc.2022.133477.

[46] S.D. Packiapalavesam, V. Saravanan, A.A. Mahajan, M.H. Almutairi, B. O. Almutairi, J. Arockiaraj, M.K. Kathiravan, S. Karthick Raja Namasivayam, Identification of novel CA IX inhibitor: pharmacophore modeling, docking, DFT, and dynamic simulation, Comput. Biol. Chem. 110 (2024) 108073, https://doi.org/10.1016/j.compbiolchem.2024.108073.

[47] V. Saravanan, B.K. Chagaleti, S.D. Packiapalavesam, M. Kathiravan, Ligand based pharmacophore modelling and integrated computational approaches in the quest for small molecule inhibitors against hCA IX, RSC Adv. 14 (2024) 3346–3358, https://doi.org/10.1039/D3RA08618F.

[48] SchrodingerLLC, Schrodinger Release 2023-1: ligPrep, 2023.

[49] L. Schrodinger, Small-Molecule Drug Discovery Suite 2023: qikProp, version 5.0, 2021.

[50] R. Kumari, V. Dalal, Identification of potential inhibitors for LLM of *Staphylococcus aureus* : structure-based pharmacophore modeling, molecular dynamics, and binding free energy studies, J. Biomol. Struct. Dyn. 40 (2022) 9833–9847, https://doi.org/10.1080/07391102.2021.1936179.

[51] V. Dalal, D. Golemi-Kotra, P. Kumar, Quantum mechanics/molecular mechanics studies on the catalytic mechanism of a novel esterase (FmtA) of *Staphylococcus aureus*, J. Chem. Inf. Model. 62 (2022) 2409–2420, https://doi.org/10.1021/acs.jcim.2c00057.

[52] R. Kumari, R. Rathi, S.R. Pathak, V. Dalal, Structural-based virtual screening and identification of novel potent antimicrobial compounds against YsxC of Staphylococcus aureus, J. Mol. Struct. 1255 (2022) 132476, https://doi.org/10.1016/j.molstruc.2022.132476.

[53] V. Dalal, P. Dhankhar, V. Singh, V. Singh, G. Rakhaminov, D. Golemi-Kotra, P. Kumar, Structure-based identification of potential drugs against fmta of staphylococcus aureus: virtual screening, molecular dynamics, MM-GBSA, and QM/MM, Protein J. 40 (2021) 148–165, https://doi.org/10.1007/s10930-020-09953-6.

[54] D.N. Gupta, V. Dalal, B.K. Savita, P. Dhankhar, D.K. Ghosh, P. Kumar, A.K. Sharma, In-silico screening and identification of potential inhibitors against 2Cys peroxiredoxin of *Candidatus* Liberibacter asiaticus, J. Biomol. Struct. Dyn. 40 (2022) 8725–8739, https://doi.org/10.1080/07391102.2021.1916597.

[55] K. Suhre, Y.-H. Sanejouand, ElNemo: a normal mode web server for protein movement analysis and the generation of templates for molecular replacement, Nucleic. Acids. Res. 32 (2004) W610–W614, https://doi.org/10.1093/nar/gkh368.

[56] B. Xu, H. Shen, X. Zhu, G. Li, Fast and accurate computation schemes for evaluating vibrational entropy of proteins, J. Comput. Chem. 32 (2011) 3188–3193, https://doi.org/10.1002/jcc.21900.

[57] R.T. McGibbon, K.A. Beauchamp, M.P. Harrigan, C. Klein, J.M. Swails, C. X. Hernández, C.R. Schwantes, L.-P. Wang, T.J. Lane, V.S. Pande, MDTraj: a modern open library for the analysis of molecular dynamics trajectories, Biophys. J. 109 (2015) 1528–1532, https://doi.org/10.1016/j.bpj.2015.08.015.

[58] A. Giuliani, The application of principal component analysis to drug discovery and biomedical data, Drug. Discov. Today 22 (2017) 1069–1076, https://doi.org/10.1016/j.drudis.2017.01.005.

[59] D. Dustin, G. Gu, S.A.W. Fuqua, *ESR1* mutations in breast cancer, Cancer 125 (2019) 3714–3728, https://doi.org/10.1002/cncr.32345.

[60] E. Paplomata, R. O'Regan, The PI3K/AKT/mTOR pathway in breast cancer: targets, trials and biomarkers, Ther. Adv. Med. Oncol. 6 (2014) 154–166, https://doi.org/10.1177/1758834014530023.

[61] K. Zhu, Y. Wu, P. He, Y. Fan, X. Zhong, H. Zheng, T. Luo, PI3K/AKT/mTOR-targeted therapy for breast cancer, Cells 11 (2022) 2508, https://doi.org/10.3390/cells11162508.

[62] R. El Botty, F. Coussy, R. Hatem, F. Assayag, S. Chateau-Joubert, J.-L. Servely, S. Leboucher, C. Fouillade, S. Vacher, B. Ouine, A. Cartier, L. de Koning, P. Cottu, I. Bièche, E. Marangoni, Inhibition of mTOR downregulates expression of DNA repair proteins and is highly efficient against BRCA2-mutated breast cancer in combination to PARP inhibition, Oncotarget 9 (2018) 29587–29600, https://doi.org/10.18632/oncotarget.25640.

[63] N.S. Sakle, S.A. More, S.N. Mokale, A network pharmacology-based approach to explore potential targets of Caesalpinia pulcherima: an updated prototype in drug discovery, Sci. Rep. 10 (2020) 17217, https://doi.org/10.1038/s41598-020-74251-1.

[64] L. Wang, C. Liang, F. Li, D. Guan, X. Wu, X. Fu, A. Lu, G. Zhang, PARP1 in carcinomas and PARP1 inhibitors as antineoplastic drugs, Int. J. Mol. Sci. 18 (2017) 2111, https://doi.org/10.3390/ijms18102111.

[65] C. Han, B. McNamara, S. Bellone, J. Harold, P. Manara, T.M.P. Hartwich, L. Mutlu, Y. Yang-Hartwich, M. Zipponi, C. Demirkiran, M.S.Z. Verzosa, G. Altwerger, E. Ratner, G.S. Huang, M. Clark, V. Andikyan, M. Azodi, P.R. Dottino, P. E. Schwartz, A.D. Santin, The Poly (ADP-ribose) polymerase inhibitor olaparib and pan-ErbB inhibitor neratinib are highly synergistic in HER2 overexpressing

epithelial ovarian carcinoma in vitro and in vivo, Gynecol. Oncol. 170 (2023) 172–178, https://doi.org/10.1016/j.ygyno.2023.01.015.
[66] S. Nowsheen, T. Cooper, J.A. Bonner, A.F. LoBuglio, E.S. Yang, HER2 overexpression renders human breast cancers sensitive to PARP inhibition independently of any defect in homologous recombination DNA repair, Cancer Res. 72 (2012) 4796–4806, https://doi.org/10.1158/0008-5472.CAN-12-1287.
[67] V.S. Patil, S.H. Deshpande, D.R. Harish, A.S. Patil, R. Virge, S. Nandy, S. Roy, Gene set enrichment analysis, network pharmacology and in silico docking approach to understand the molecular mechanism of traditional medicines for the treatment of diabetes mellitus, J. Proteins Proteom. 11 (2020) 297–310, https://doi.org/10.1007/s42485-020-00049-4.
[68] X. Huang, H.M. Rehman, A.G. Szöllősi, S. Zhou, Network pharmacology-based approach combined with bioinformatic analytics to elucidate the potential of curcumol against hepatocellular carcinoma, Genes (Basel) 13 (2022) 653, https://doi.org/10.3390/genes13040653.
[69] H. Masuda, D. Zhang, C. Bartholomeusz, H. Doihara, G.N. Hortobagyi, N.T. Ueno, Role of epidermal growth factor receptor in breast cancer, Breast Cancer Res. Treat. 136 (2012) 331–345, https://doi.org/10.1007/s10549-012-2289-9.
[70] S. Priyankha, M. Prakash, Evaluation of the efficacy of marine natural products against PARP-1/2 proteins in high-grade serous ovarian cancer: insights into MD and SMD simulations, J. Biomol. Struct. Dyn. (2024) 1–15, https://doi.org/10.1080/07391102.2024.2335290.

View publication stats